PROCESS METRIX
Instrumentation for Process Control

6622 Owens Drive
Pleasanton, CA 94588
Voice: (925) 460-0385
Fax: (925) 460-0728

Final Report

Award Number: DE-FC26-03NT41969

Project Title: "A High Speed Laser Profiling Device for Refractory Lining Thickness Measurements In a Gasifier with Cross-Cut to the Metals, Forest Products, Chemical and Power Generation Industries"

Reporting Period: December 1st, 2004 – October 31st, 2007

To: Jenny Tennant
National Energy Technology Laboratory
3610 Collins Ferry Road, P.O. Box 880
Morgantown, WV 26507-0880

Principal Investigators:

Process Metrix	–	Michel Bonin, Tom Harvill, Jared Hoog, Don Holve, Alan Alsing
Acuity Technologies	–	Bob Clark
Eastman Chemical Company	–	Steve Hrivnak

DISCLAIMER

Table of Contents

List of Figures

List of Tables

1. PROJECT OVERVIEW AND MOTIVATION

Within the metals, forest products, power generation (gasification) and chemicals (also gasification) industries there are opportunities for enhanced process optimization using high-speed laser profiling devices. Gasification and integrated gasifier/fuel cell (IGFC) systems are of particular interest. They represent an integral component of DoE/FE's Vision 21 program, which will revolutionize the power and fuels industries by developing systems having no net CO_2 emission or adverse environmental impacts. First generation laser profiling instrumentation intended for use in these industries were developed as general purpose tools, expected to adapt to a range of functions spanning architectural engineering reverse analysis, urban planning, power transmission line assessment, etc. as well as the aforementioned process applications. Early instruments were expensive and slow causing lost product throughput because of the instruments' limited data acquisition rate.

With the advent of low cost, high-power diode lasers, high-speed range finding technology has reduced the time required to collect profile information and improved the accuracy and robustness of the instrumentation. However, these profiling devices remain generalized in design and adaptation. They perform well in non-demanding environments where they can be operated at ambient temperature, the field of view requirements are flexible, and the accuracy requirement not particularly stringent. Their primary limitations derive from the integrated scanner/range finder design embodied in these state-of-the-art laser-profiling instruments. However, the industrial applications noted above require a low cost instrument that can be easily adapted and configured for the geometric and environmental conditions specific to each industry. This requirement forms the basis for the project: The development of a scanning laser range finder that can determine the profile of a process device or product and that enables cross-cutting application for process optimization, energy savings, and control for product quality in basic commodities industries (metals, chemicals, forest products) where similar profiling capability is also needed. However, to enable a manageable program scope, the gasifier was selected as the first application for initial instrument development. This approach was based on several factors that include:

- Gasification and integrated gasifier/fuel cell (IGFC) systems are an integral component of DoE/FE's Vision 21 program, which will revolutionize the power and fuels industries by developing systems having no net CO_2 emission or adverse environmental impacts.
- Our prior success in this environment (though of limited coverage, see Figure 2),
- The critical need for lining thickness measurements in this industry,
- The potential for gasification as an efficient and environmentally benign provider of chemicals and power,
- The fact that this represents one of the more challenging applications (the remaining applications then become a simplification of the first) and,

- The commercial potential of the successfully developed instrument (there are approximately 80 gasifier world-wide, with additional units under construction).

Since the vessels used in the steel industry are open-mouthed, access to the vessel interior in these applications can be made from a standoff distance of 10-20 feet without sacrificing field of view into the vessel. For the gasifier application, the burner/access port is typically less than two feet in diameter, and up to 48" long. In this geometry, only the lower portion of the gasifier is in the field of view of the instrument.

Figure 1 illustrates the available field of view for a ranging/contouring instrument placed as close as possible to the external face of a short (24" long) gasifier burner port. For a long burner port, such as the 48" configuration at Eastman, the field of view available from the external face of the burner port is so small that it precludes collection of any useful data from this location. In order to view the gasifier dome, a down-hole device that is capable of withstanding high thermal loading is required. The same criteria apply to any narrow-entry geometry such as the AOD and de-gasser vessels used in the steel industry to produce stainless and low carbon content steel, respectively. BOF and ladle applications also require a small, compact head (close-coupled scanner and range finder) that are externally shielded against the high radiative heat loads.

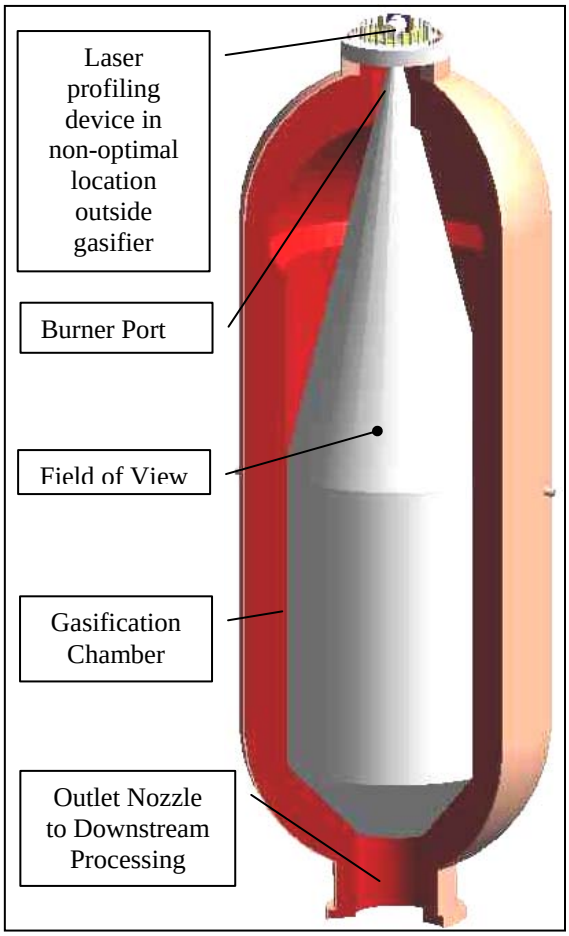

Figure 1. Typical gasifier illustrating the field of view (measurable refractory) that results from centerline measurements made with the ranging (contouring) instrument located immediately adjacent to the burner port. A customized instrument is required that can obtain range measurements throughout the gasifier, including the upper section and dome.

For broad applicability to the industries cited above, a suitable range finder must be capable of satisfying the following requirements:

- Accuracy – 1-2 mm over maximum range of 20 m,
- data acquisition rate - 2-10 KHz,
- fast measurement time – 1-2 minutes per acquisition to minimize thermal load on

mechanical components in high temperature environments, 1-2 seconds to optimize production efficiency in some applications,

- flexible scanner configuration capable of trading off scan speed, point density, and field of view,
- surface ambient light and radiation – must be capable of accurate measurement on radiating surfaces up to 3000 °F, or on fully sunlit surfaces.

To fully realize the potential benefits of high performance scanning range finders across multiple industries, high sample rate range finder performance must be improved over the existing state-of-the-art. This forms the basis of the work described herein.

2. TECHNICAL DEVELOPMENT

2.1. Definition of the Range Finder Configuration

2.1.1. Wavelength Considerations

The High Temperature Ranging System (HTRS) range accuracy requirements for the gasification application are ± 3mm best case, with the maximum peak-to-peak allowable uncertainty of ± 25 mm. Various range finder technologies were reviewed relative to their ability to achieve these accuracy requirements. The primary concern is creating a ranging system having sufficient energy to overcome the high background expected from a hot surface. Several possibilities were evaluated, all based on the existing modulation technique employed by Acuity Technologies in their current line of commercial sensors (e.g. AR-4000):

Several modifications to the AR-4000 configuration were considered. These included:

1) Shifting the laser wavelength from the red (670 nm) laser used in the AR-4000 to the blue (405 nm).

Advantages:	-Background light is reduced by a factor of 190.
Disadvantages:	-The only manufacturer of blue laser diodes offers a 405 nm laser that produces ~30 mW of output power. This may not be sufficient. -The diode is expensive ($5K) and has shorter lifetime compared with those available at 670 nm.

2) Shifting the laser wavelength from the red (670 nm) laser used in the AR-4000 to the green (532 nm) and using a frequency doubled Yttrium Aluminum Garnet (YAG) laser or diode pumped laser, both of which are available at higher power.

Advantages: -Background light is reduced by a factor of ~7 compared with the background light at 670 nm, but increases by a factor of ~28 compared with the background light at 405 nm.
- There are numerous manufacturers of YAG and or diode pumped lasers, (Lumanova, Alphlas, Arctic Photonics, Teem Photonics, QPeak, Cryals, Crystal Laser), and the product would not be dependent on a single supplier.

Disadvantages: -The YAG is operated either in CW mode (always on) or in pulsed mode. Pulse mode requires a Pockel cell. Operating the YAG in a modulated light configuration will require a Pockel cell. Although Pockel cells are used frequently in the laser science industry, this device has not been evaluated for adaptability in the present application, and thus represents higher risk.
-An analysis is required to determine if the power availability of the YAG lasers will yield a sufficient signal-to-background signal.
-As shown below, the presence of particle fields severely retards accuracy at short laser wavelength.

2.1.2. Background analysis at 532 nm

The background radiation at 532 nm is 28 times that at 405 nm. Therefore, 600 mW of power is required at 532 nm to achieve the same signal-to-background ratio obtainable with a 20 mW laser operating at 405 nm.

For a first order estimate, assume the energy flux though the lens onto the detector comes from a region two times the diameter of the lens, and the baffling is sufficient to eliminate oblique radiation. This might be conservative, as careful control of the optics combined with a pin hole aperture could restrict the collection area to that just slightly larger than the lens. Nevertheless, assuming the following:

- a conservative collection area 70 mm in diameter (or and area of 3848 mm^2),
- a surface at nominally 1500 °C
- a surface emissivity of 0.8,
- a center wavelength of 532 nm,
- and a 2 nm wide band pass filter,

the relevant flux from the surface that passes the optical band pass filter can be calculated. First, using the parameters above, from Planck's Law the emission from the surface is (1,718 W/m^2-μm). The amount of energy passed by the band

pass filter over the collection area is given as (1,718 W/m^2-μm)*2 nm/(1000 nm/μm) * 3,848E-6m^2 = 13.224 mW.

At 1 m minimum measurement range (the worst case scenario for this analysis), the hemispherical area that the surface emission diffuses over is 2*pi*1m^2. That gives a lens/ diffuse area ratio of 962E-6/6.28 = 1.53E-4. Thus, the best estimate of total collected background emission through the optical system is 13.224mW*1.53E-4 = 2.026 uW.

Incorporating a 532 nm laser operating at 200 mW (the highest common 532 nm available) and a surface reflectivity of 30% and hemispherical scatter of the incident laser energy, the total amount of laser light collected by the optics is on the order of 1.53E-4*0.3*200*1000 = 9.2 uW. This yields a signal-to-background ratio of approximately 4, which we consider an insufficient margin.

A less conservative optical system could be achieved by weakly focused receiver optics. Assuming the surface spot size can be reduced to that of the lens (35 mm) and following the analysis above increases the signal to background to ~16. A few YAG lasers are capable of 600 mW output, which increases the signal-to-background to 48, an acceptable margin.

Although this system appears to provide acceptable signal-to-background, the Pockel cell modulation approach is untested. In lamp-pumped laser systems, there is 3-5 ns of jitter in the time delay between the q-switch firing and the time that light actually exists the device. This level of jitter would lead to unacceptable range error if used in conjunction with the modulation scheme embodied in the AR-4000 system. In addition, at 600 mW of power, there may be laser safety issues to consider, though these would be mitigated by the scanned beam and containment by the gasifier interior.

2.1.3. Background analysis at 405 nm

Assuming the high-efficiency receiver optics, a system operating at 405 nm with 20 mW of power should yield the same performance as one operating at 532 nm with 600 mW of power. This would seem attractive, and we thought so as well, until we calculated the number of actual photons that would arrive at the detector assuming a modulated power level of 20 mW from the blue laser. These calculations predict only 1.6 photons arrive at the detector per ns, which is insufficient for the modulation scheme to operate reliably. The AR-4000 expects ~20 photons per ns, and we estimate that at least 100 photons per nanosecond are needed (minimum) to overcome the background expected in this application. Thus, we have concluded that the low power, 405 nm laser configuration is no longer an option.

2.1.4. Time-of-flight ranging

While we explored the high-powered YAG option, changing the range measurement approach altogether and incorporating a recently developed laser technique was also a possibility. Microchip lasers have been developed over the past 10 years that have the capability to deliver high peak power (kW levels) over a short, <1 ns pulse widths. These systems typically operate at 532 nm, are small, compact and offer excellent reliability. This laser, coupled with conventional time-of-flight measurement capability, completely eliminates any signal-to-background concerns because of the high peak-power involved. The tightly collimated laser beam also enables small scan mirrors. Initially, we believed that an ultra-fast timer having better than 50 picosecond time resolution was required, and that this timing solution was available in both a chip- and module-level forms off-the-shelf. However, as shown below, our 50 ps error estimate for the timing circuit alone was an order of magnitude too high which negated the utility of any of the off-the-shelf solutions we were considering at that time.

After additional review of the analysis above, Acuity Technologies and Process Metrix concluded that a laser operating at 405 nm having sufficient power to excite the detector in the AR-4000 simply did not exist. This was an unfortunate conclusion, necessitating a shift in range finder technology from the modulation approach embodied in the AR-4000 to more traditional time-of flight technology.

Realizing that time-of-flight ranging would be needed, in early December 2005 Acuity Technologies investigated the feasibility of developing a microchip laser-based ranging system operating on the time-of-flight measurement principle. This investigation determined the following:

- Microchip lasers are being manufactured by JDS Uniphase and Northrup Grumman/Synoptics under license from MIT,
- A field of use restriction exists on the MIT license, preventing use of the microchip laser for ranging purposes,
- A company called Cyra Technologies, owned by Lieca Geosystems, owns the field of use rights for microchip lasers applied to ranging systems,
- Cyra also has a number of patents that restrict range timing to faster than 30 ns.

Thus, before we felt comfortable moving forward with a microchip laser-based range finder, we deemed it necessary to determine whether or not Cyra would be willing to license their field of use rights and range timing IP to us for application in hot surface contouring systems.

In early January 2004, we (Process Metrix and Acuity) met with Greg Walsh, Director of Engineering for Cyra Technologies. After meeting with Mr. Walsh, he subsequently met with the CEO and CFO of Cyra, who both agreed to provide the requested license to Process Metrix. In advance of the license, Cyra instructed JDSU to provide Process Metrix with up to five lasers for research and development purposes and an order was placed for two units.

2.1.5. Particle Scattering Sensitivity

The high power of the laser pulse has the potential to illuminate particles of dust suspended in the beam path between the laser and the far reflecting surface. Could the range measurement be swamped by ambient dust loadings?

The outgoing laser pulse for typical microchip lasers is between 400-1000 ps wide. As this pulse encounters particles, radiation backscattered by the particle field can potentially exceed the detection threshold of the receiver and result in a false range measurement. After the laser pulse reaches the reflecting surface, much of the energy is absorbed (at least for the surfaces we're anticipating in the gasifier application). Assuming gray body behavior, the reflected energy is scattering into a hemisphere, and the return energy is 6-8 orders of magnitude lower than the incident energy. Thus, any particle scattering that occurs as the reflected pulse returns through the particle cloud will be small. Furthermore, photons scattered by particles interacting with the return pulse will arrive at the detector at the same time as the primary reflected pulse. Therefore, there is no detrimental contribution from particle scattering by the return pulse.

Because there is the potential for range error associated with the outbound laser pulse, two signal processing algorithms should be included in the electronics/firmware. The first is thresholding the input signal to prevent low level signals from falsely triggering the range measurement. This capability has already been built into the detection electronics, though tuning of the threshold can only be accomplished by changing discrete components. The second involves first/last pulse processing. Since we know from our qualitative analysis above that the last pulse detected for a single laser event must be that from the far field surface, configuring the instrument firmware to only detect the last pulse in a timing window corresponding to the maximum target range should mitigate particle effects to an acceptable level. The challenge with this approach occurs when the particle cloud is in close proximity to the target surface. Under these conditions, it may be difficult to separate particle scattering effects from wall effects. Fortunately, near-wall particle clouds are often at longer range where particle back-scattering is reduced by the square of the distance between the particles and the detector.

2.2. First Considerations for a Time-of-Flight Range Finder Electronics

Needless to say, when the project plan was first assembled, we did not anticipate these complications and several months project time were expended in determining the proper route forward with regard to the ranging solution. We remained confident that this approach would be reasonably low-risk from the technology development perspective, though the transmitter/receiver technology to drive the laser and time the signals would now have to be developed.

Acuity Technology agreed to take on this responsibility, incorporating an off-the-shelf timer chip that has been recently upgraded to much faster performance. The range finder development was ultimately segregated into three individual circuit boards:

1) **PCI Interface card:** This board is located in the computer that drives the range finder, and communicates and controls the range finder, as well as the encoders that define the mirror positions of the scanner. The board can capture data at full speed or better, 20,000 samples per second, and transmit it to an application program written in C.

2) Photodiode receiver card: The board detects and amplifies pulses reflected from the ranging surface.

3) GPX time measurement chip: This chip resides on a daughter card attached to the PCI interface board, and receives start and stop signals from the receiver. The chip measures the time between the start and stop signals. During the development period, the supplier of the high speed timing chip informed us that they had received and successfully tested the first silicon of a new higher performance chip. Based on their test results, we decided to modify the design of the main timer card to use this IC rather than the previous generation, to take advantage of the reduced time error of the faster IC.

2.3. Evaluation of Prototype Time-of-Flight Range Finder Electronics

In December 2004, Process Metrix met with Acuity Technologies to view a demonstration measurement of range off of a target placed approximately 30m from the transmitter/receiver. The receiver card was fully functional, and incorporated a 300 um diameter photodiode. A beam expander in the transmit beam was necessary to address the unexpectedly high beam divergence of the JDSU laser. The beam expander results in a collimated beam output of approximately 25 mm diameter. A small pick-off window in the transmit beam

path deflects a small (less than 2%) amount of laser energy to the detector to temporally mark the outgoing beam.

The return pulse was collected by a 35mm lens having a focal length of approximately 100 mm. Using this system, we observed the following:

- The outbound laser pulse rate is approximately 12 kHz, and seems stable and repeatable,
- The return pulses measured from a white, cardboard target are equally stable,
- Small movements in the position of the target were easily discernable,
- Pulse noise was evident. For this non-optimized optical geometry, the current noise level is estimated to be approximately 5-6 mm. Acuity anticipates reduction in noise after improved optical and electronic filtering,
- The first revision receiver board was working well. A second revision may be needed before finalizing the design,
- Although a silicon photodiode was used for the demonstration, we agreed that an Avalanche Photodiode (APD) would be required for the final version system to enable pulse detection at extended range. Switching to the APD will require the addition of an APD power supply card; a provision that Acuity has already accommodated in the board design,
- Removing the beam expander (a non-optimal collimator) from the beam path severely degraded performance. Therefore, it was clear that the high beam divergence of the JDSU laser will require beam expansion and collimation to preserve acceptable signal-to-noise ratios. This has been incorporated in the transmitter design (see below).
- A method for mounting the receiver board using a 3-axis positioning system will be required. This has been incorporated in the transmitter design (see below).
- The receiver lens geometry should be configured to yield a 150 um spot size,

- The JDSU laser power supply has to be reduced in size, and configured to operate on 12-24 V.

Miscellaneous Issues

- The PCI card was working well,
- The system will have to pass CE certification. Electronic design has been undertaken assuming this testing will be needed. Pre-testing will be done when the entire unit has been packaged,
- A board level computer and three-slot backplane will be housed in the turret base of the scanner. It will be PMC's responsibility to program the computer based on documentation received from Acuity that describes the range finder control logic.
- Smoke effects: This was discussed in the context of the pulse train expected when there is smoke between the range finder and the surface of interest. Acuity has built in the capability to report last pulse timing, e.g. pulse reporting of only the pulse originating from the surface of interest, assuming there remains sufficient laser power to a) penetrate the smoke and reach the target.

2.4. Optical Design of the Scanner

The overall scanner design for gasification applications is illustrated as a three-dimensional CAD model in Figure 2. The upper portion, or turret, is the only portion of the instrument that will be exposed to the heat load. The turret enclosure is water cooled, and constructed from a single wall annulus with cooling supply and return points at the bottom and top of the enclosure, respectively. The turret is hermetically sealed, allowing its interior to be flushed with N_2 during assembly, eliminating condensation accumulation on optical surfaces. The lower portion, or turret base, will be inserted in a secondary water cooled, hollow cylindrical mount (not shown). This "positioning mount" serves to shield the cables and cooling lines tied to the instrument from the hot walls of the gasifier inlet throat, as well as position the instrument at a known location in the gasifier by mounting externally on the gasifier flange.

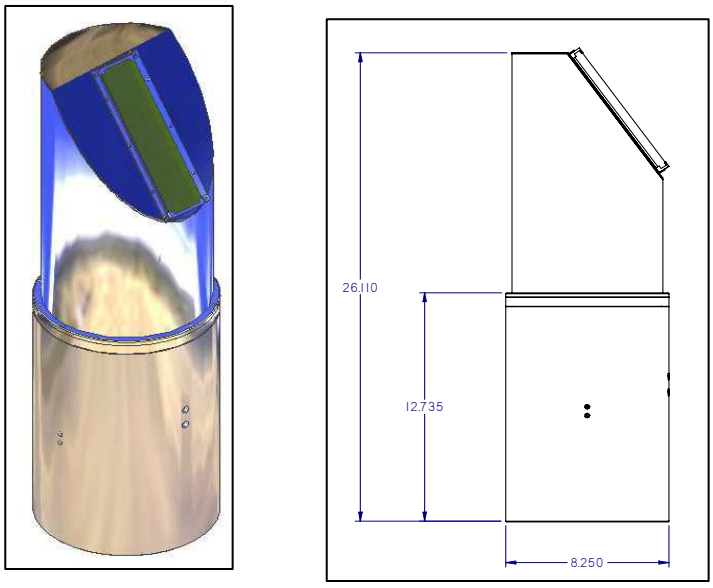

Figure 2. Gasifier lining thickness measurement instrument – external view. All dimensions in inches.

The internal components of the system are illustrated pictorially in Figure 3. The primary interface to the system will be through an Ethernet interface, the only facilities necessary to operate the system include:

- Ethernet communications
- 12V Power
- Cooling water.

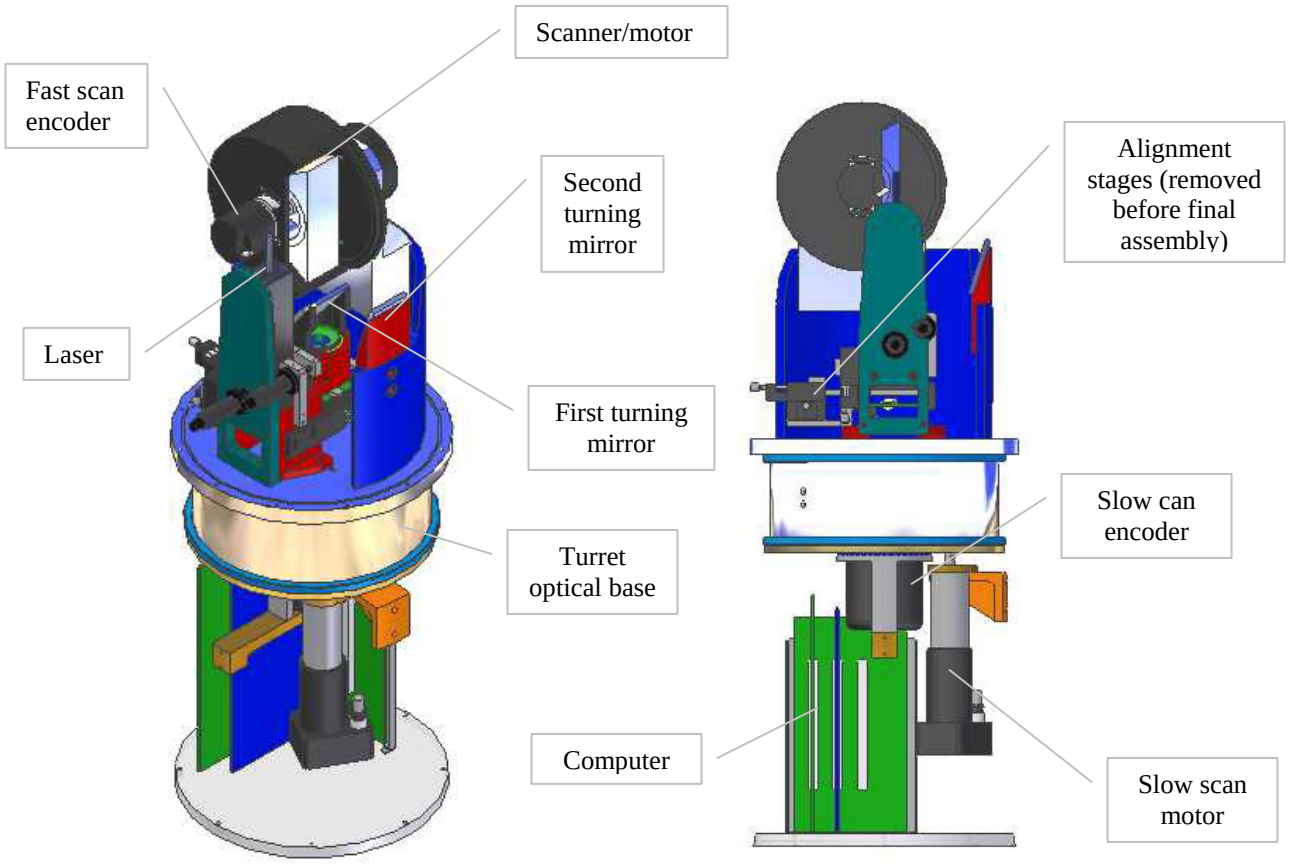

Figure 3. Internal components of the gasifier lining thickness measurement system.

After all of the mechanical parts were received from the machinist, they were assembled and optical performance of the transmitter/receive evaluated. A photograph of the transmitter/receiver are shown in Figure 4.

The optical assembly is functions as designed. Minor modifications were required to some of the parts to facilitate alignment, but otherwise we observed a collimated beam diameter of approximately 5.5 mm, as predicted by optical modeling performed earlier in the project. In addition, should we decide that a focused beam be more appropriate for some applications, we can easily change the position of the negative lens relative to the final focusing lens to focus the beam at a specific distance from the transmitter. This operation could even be

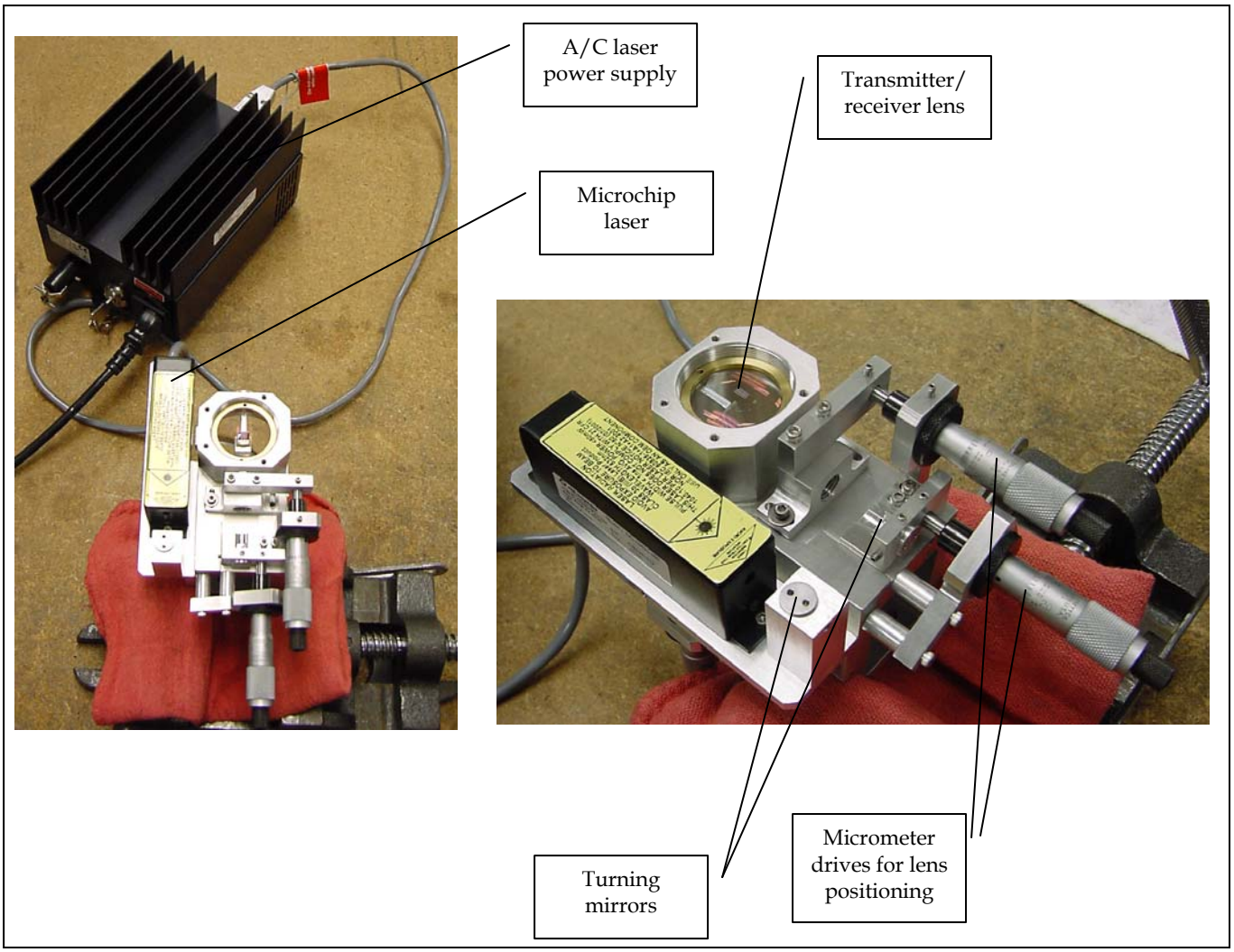

Figure 4. Transmitter/receiver optics and A/C powered laser configuration for testing and evaluation of transmit optics.

configured for on-the-fly adjustment by replacing the manual micrometer drive with a piezo-electric drive, and adding a translation stage to the lens mount. We may find this configuration useful if detailed measurements of small areas in the gasifier are needed.

Photos of the turret mounted to the turret base of the assembly are presented in Figure 5. The principle concern was the tolerance between the turret bearings and turret mount. The machine tolerance for the mounting surfaces at the bearing location is ±0.0002, well beyond the standard tolerances that most machine shops can hold. We were pleased and gratified to find that after moderate heating of the turret base and cooling of the turret, the entire assembly

slipped together without difficulty. The rotation of the turret on the base is smooth and even.

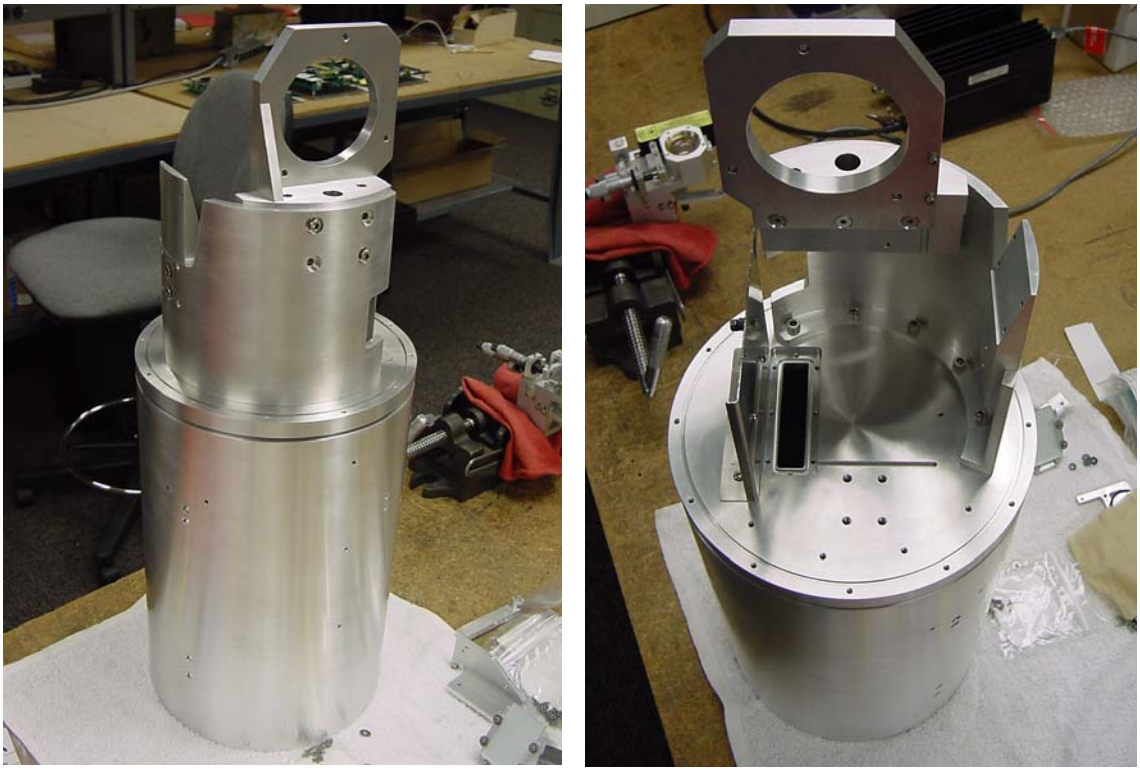

Figure 5. The turret and turret-base assembly.

2.4.1. Optical Layout

The optical geometry of the system is illustrated in Figure 6. This section view includes the collection lens, scan mirror, turning mirrors and slow scan encoder, as well as the optical base and cooled enclosure (note that annulus). Three orientations are shown for the fast scan mirror: The original orientation (in black), the start scan orientation (in green) and the end scan orientation (in red). The blue lines represent the marginal and centerline ray traces from the lens aperture to the mirror. The optical layout required requires two additional turning mirrors to effect scanning from -1.6° to +92° for a total scan angle of 93.6° (note that the 0° direction represents the horizontal plane). The three-sided scan mirror has a facet dimension of 100 x 33 mm.

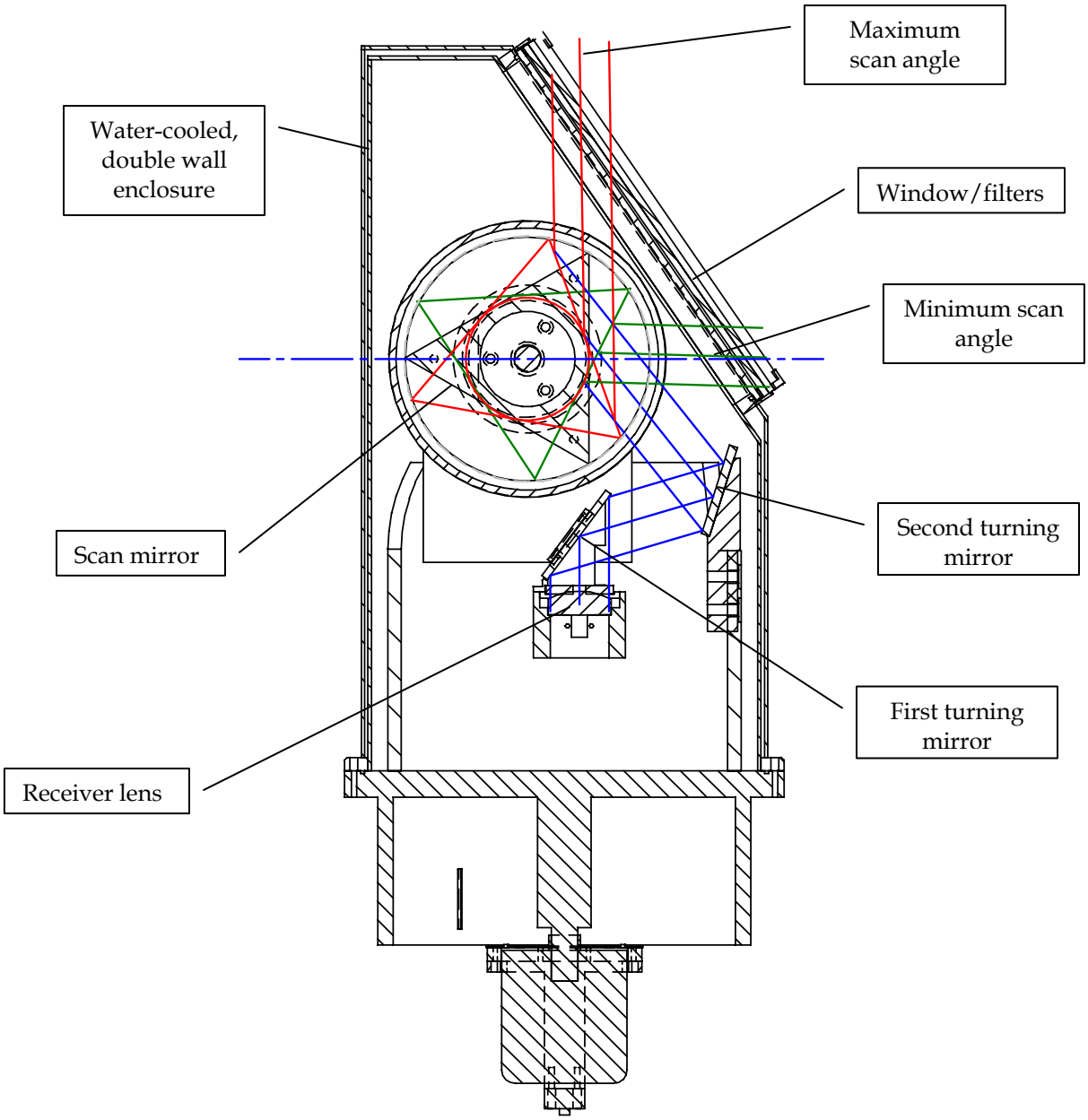

Figure 6. Optical layout of the gasifier lining thickness measurement system.

In practice, the instrument will be inserted into the gasifier upside down, and the scan angles noted above will allow coverage of the entire gasifier interior as the turret is rotated through 360°.

One of the critical issues associated with the optical design is to prevent specular reflections of the transmit beam off of optical surfaces in the beam path from reaching the detector. Although AR-coated, each window surface in the beam path can potential reflect 0.3-0.5% of the incident laser energy. Assuming 2 kW of pulse energy, this equates to 5-10 W of light which, at a minimum insert

unacceptably long detector recovery times in either the detector or amplifiers, or worse, shorten the lifetime of the avalanche photo diode (APD) detector.

Specular reflections from windows can potentially reach the APD at or near 0° scan angle. Although most of the energy should be reflected back towards the laser by the last turning prism in the beam transmit path, any diffusion of this relatively high intensity light the windows are tilted through 15°. This deflects specular reflection off of the fast scan mirror, preventing them from propagating to the detector.

The second, more egregious condition occurs when the scan mirror face is nearly normal to the beam as it exits the transmitter assembly. In this orientation, ALL of the transmit beam can be potentially reflected back to the APD; a condition that would most assuredly damage the APD. The laser timing requirements are described as follows:

Scanning is accomplished using the aforementioned three-sided, rotating mirror, which rotates at 200 RPM (3 RPS) for the lowest resolution measurements. For each rotation of the mirror, the laser must be turned off for a portion of the rotation to avoid back-reflecting the output beam into the receiver. Doing so will damage the detector.

Since the encoder pulses that describe the fast-scan mirror position are introduced directly into the Acuity board, the FPGA on the Acuity board must be configured to provide a laser on/off signal.

The laser has a control input that can be used to turn the laser on and off. There is some uncertainty regarding the warm up time of the laser before stable operation is obtained that could affect maximum power output or pulse repetition rate stability. We completed the evaluation of laser on/off timing that could critically affect the maximum throughput rates for the range finder. The fastest rotation rate needed to achieve the lowest scan resolution is only 200 RPM. Using this new maximum rotation rate, the timing values are as follows:

1) Mirror rotation period: 300 ms
2) Laser on during scanning; 33.3 ms
3) Laser off to blank receiver: 28.9 ms
4) Available latency to turn the scanner on, and prepare for the following scan: 37.8 ms. After this latency, the laser must be up and pulsing again at full power, with stable repetition rate.

The laser has an external input that can be used to cycle the laser on/off three times during a single rotation period of the fast scan mirror. When the laser is

on, it is still pulsing at 12 kHz. A function generator set to produce a square wave becomes a simple laser on/off controller when connected to the lasers external input. A high speed photo diode was used to detect the individual laser pulses, with the output from the diode and the function generator observed on a 100 MHz oscilloscope.

Several waveforms that describe the performance of the laser are illustrated in Figures 7-9. Figure 7 shows once complete cycle in which data would be collected, the laser turned off to avoid detector damage, the laser turned on again in preparation for the next acquisition cycle, and then the next acquisition cycle.

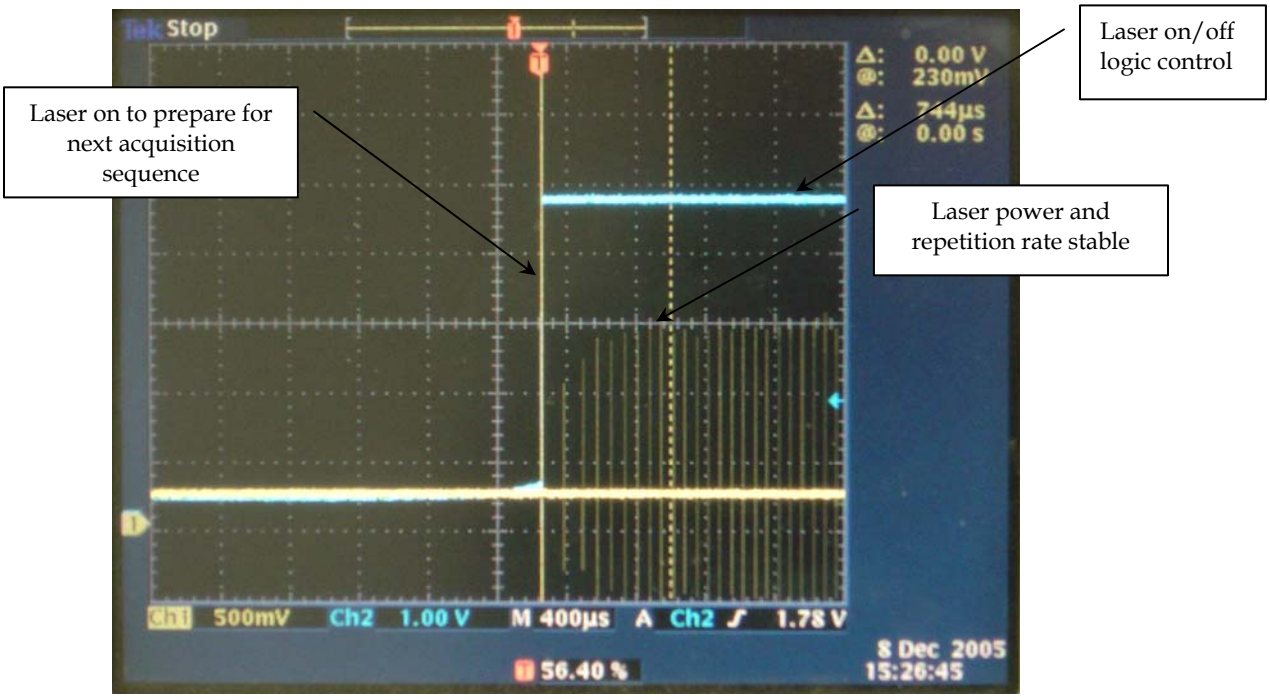

Figure 7. Screen shot of oscilloscope showing laser on/off logic pulse (light blue trace) and laser pulses (yellow trace).

Figure 8 illustrates the detailed startup transient that occurs as the laser is turned on after the blanking period. Clearly, there is variability in both the pulse amplitude and repetition rate at early times of the start up sequence. However, after 7-9 pulses, the laser is again operating in a stable mode that can be used for data acquisition. Within the latency period of 37.8 ms, there will be ~450 laser

Figure 8. Detail view of laser startup transient after laser-on logic pulse. Laser operation is stable after approximately 7-9 laser pulses.

pulses; more than enough to stabilize laser operation before data acquisitions begins. Figure 9 illustrates the detailed view of the laser-off logic pulse.

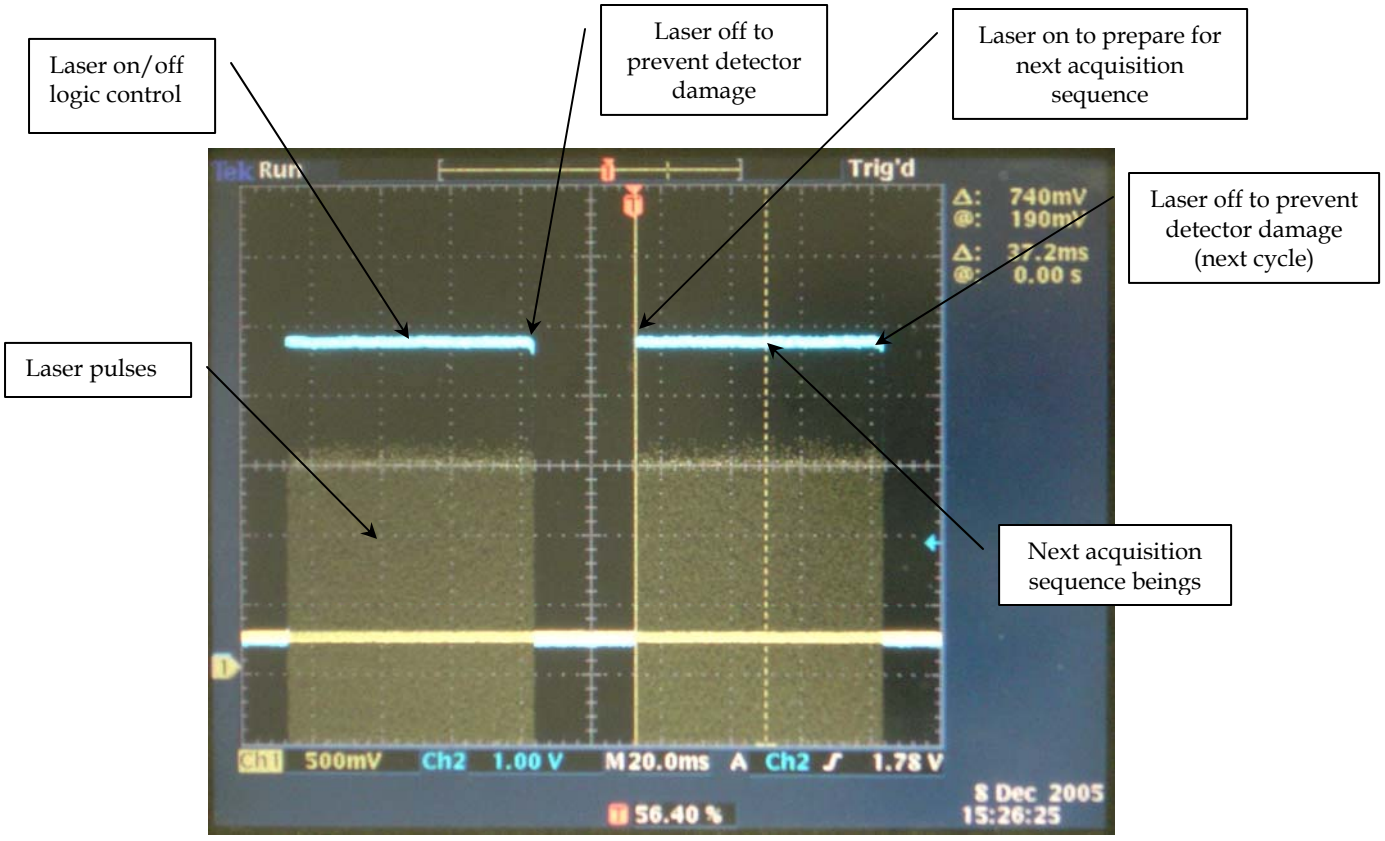

Interestingly, the laser emits 2-3 additional, random pulses after the logic pulse goes low. Knowing that these exist requires careful control of the laser-off timing to ensure that no light emitted directly from the laser reaches the detector.

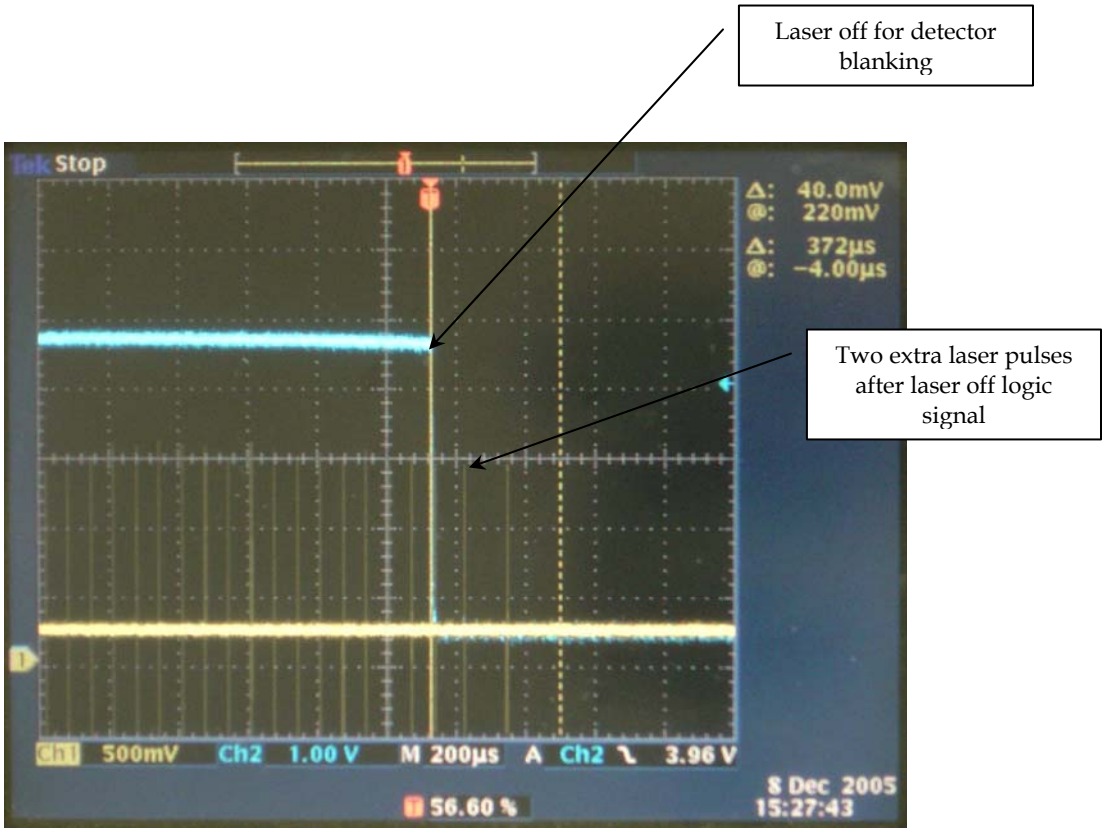

Figure 9. Detail view of laser shut down transient after laser-off logic pulse. Two-three laser pulses typically occur after the shut down logic pulse.

2.4.2. Cabling and cooling lines between turret and turret base

Numerous electrical connections are required between the turret base (stationary component) and the turret. At the suggestion of Bob Clark (Acuity), we concluded that the best method of interfacing the electronics between the turret and the turret base is through a flat, flexible cable (FFC). This type of cable is often used to connect the moving print-head on an ink-jet printer to its stationary base. Manufactured using methods similar to those employed to construct a printed circuit board, The (FFC) will have to be custom design to carry the number and type of signals between the turret and turret base. Custom electronics boards and sealed connectors will also be fabricated to interface the FFC to the turret and turret base connection points.

In operation, the FFC will wind, and then unwind as the turret rotates through 360°. Note that on power up, the system will be configured to return to the same home position (rotation) to avoid over-winding the FFC. We've included a

geared, multi-turn potentiometer in the turret to allow an absolute measure of turret position. This will allow the system to always return to the same home position, even if power to the unit is turned off in the middle of a scan.

The head includes and integral, water-cooled turret enclosure. After struggling with a design to route the cooling water for the turret enclosure through the internals of the scanner, we elected to eliminate the internal routing, and implement external cooling lines. Should there be a leak in the system, this approach prevents the possibility of bringing water in contact with the internal electronics. It also eliminates the need to coil and un-coil the water lines as they transition from the turret base to the turret. Of course, the water lines will now have to coil around the exterior of the cooling jacket. This is not an ideal solution, but a manageable one preferable to internal routing.

2.4.3. Instrument Calibration

Instrument calibration of both range and beam position is a critical factor that must be addressed. Some facility for calibration has to be built into the scanner, which follows from the original list of design goals/constraints. We have incorporated multi-axis translation and rotation into the transmitter beam launch optics to facilitate accurate setup of the transmitter beam. Beam pointing is critical: the beam location on the surface must be known to an accuracy of ±1-2mm, which implies a pointing stability of better than 10 arc seconds at a distance of 12 meters. These accuracy requirements have impact on the following design elements:

1) Optical properties of the scan mirror: Within the project Process Metrix has worked closely with Lincoln Laser, the predominate manufacturer of rotating scan mirrors for laser scanning applications. Their high accuracy, diamond-turned mirror meets or exceeds the necessary design parameters. The overall design goal is to minimize the face-to-face angular uncertainty, holding a tolerance of better than 10-20 arc seconds. This is necessary to ensure accurate beam pointing, independent of range accuracy.

While 10-20 arc second planarity is achievable for a diamond-turned mirror it is a greater challenge to source a motor/encoder combination that has shaft run-out on the order of 10-20 arc seconds available in a package size that satisfies the design constraints we have established. After several iterations, we settled on a motor/bearing combination manufactured by Lincoln Laser coupled with an encoder from Heidenhain, one of the most reputed encoder manufacturers available. By allowing Lincoln Laser to supply motor, bearings and shaft, we are assured of a mirror/motor combination that meets the pointing specifications noted above. The Heidenhain inclinometer is an integral bearing unit (we also

reviewed bearingless, shaft mounted encoders but concluded that these models did not have adequate accuracy), allowing a simple mounting geometry and a rated accuracy of 12 arc seconds.

The first quotation for the scan mirror from Lincoln Laser was unacceptably high ($5,500 NRE + $8,700 for the mirror in single quantities). PMC and Lincoln Laser worked together to address the cost of the scan mirror, which is driven by a number of parameters, including facet size. To reduce cost, PMC has redesigned the optics to reduce the required facet size from 100 x 33 mm to 75 x 33 mm. In addition to reducing costs, the mirror size is compatible with other scanner requirements at PMC, allowing multiple unit pricing as PMC orders identical scan mirrors for multiple platforms.

2) Encoder resolution: The encoders selected for both the scan and turret drives have resolutions of 0.025 arc seconds; significantly more than needed to achieve the design goal.

3) Laser pulse timing against mirror position:
This parameter will be measured and accounted for in software.

4) Laser/receiver alignment: To simplify the scanner design, we have designed around a single scan mirror that reflects the outgoing beam to the surface, and the reflected beam from the surface back to the detector. Our objective (which as achieved) was to incorporate both the laser and receiver into a single, monolithic block that can be aligned as an ensemble. Alignment in the scan plane (i.e. in the line scan direction) will be accomplished via software. Alignment perpendicular to the scan plan must be accomplished at system setup by tilting the transmitter/receiver assembly. This capability was also designed into the assembly.

5) Mounting stability of the system: Mounting stability can be subdivided into two elements: a) The stability and reproducibility of the external instrument mount and b) the stability of all internal mounts, with the latter including thermally induced expansion and contraction. The monolithic character of the transmitter and receiver minimizes thermal issues, while the design itself must include appropriate mounting and adjustments for alignment purposes.

6) Minimum stand-off distance: The standard system developed by Acuity has a reset time of 6 ns. Since the same circuitry is used to mark the start and stop points of the timer, this reset time is unavoidable. Therefore, the system using the current electronics will have a minimum standoff distance of approximately three feet, *measured from the last optic (e.g. the window) in the optical path.* For the

Eastman gasifier, this means that unless we find a method of reducing the reset time, we will be unable to measure the upper cone of the gasifier.

7) Calibration Fixtures: To test and configure the range finder to the aforementioned beam pointing constraints, we designed and had our machinist fabricate the necessary fixtures needed to calibrate the mirror position of both the fast and slow scan axis. Two fixtures were designed and constructed: One to accurately position the laser system adjacent a Helium Neon (HeNe) pointing laser, and a second to mount two detectors at a known distance from the range finder. The two fixtures are illustrated in Figures 10 and 11.

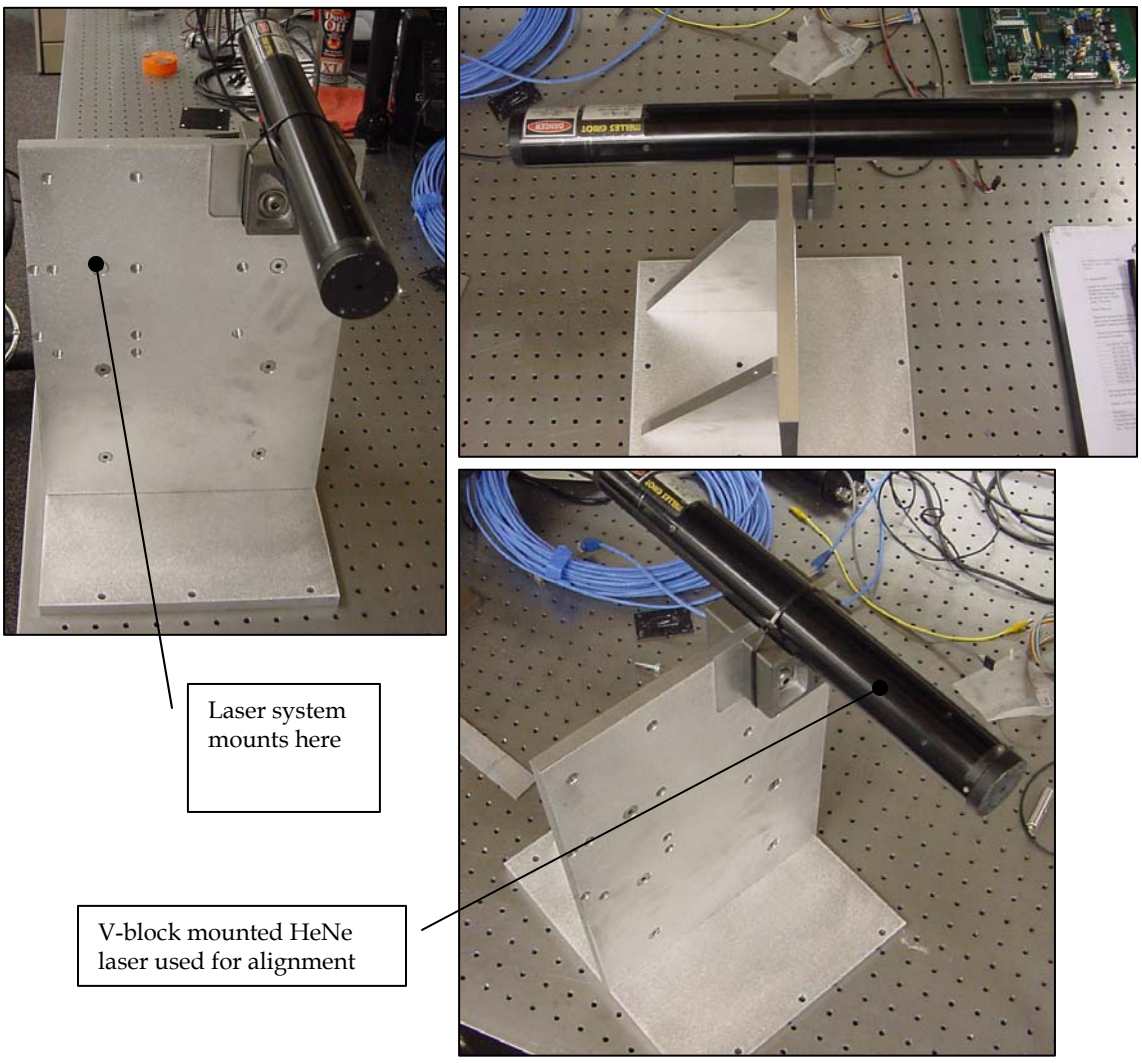

Figure 10. Calibration fixture used to position laser system and separate pointing laser in known positions.

We are targeting pointing accuracy (i.e. where the beam is on the target surface) of 0.25" at a range of 50'. This equates to an angular accuracy of ~400 micro-radians. Thus, the accuracy of the pointing laser must be as good, or preferably better to ensure that the pointing accuracy of the laser scanner is within the target range.

The pointing stability of the HeNe can easily be determined by rotating the laser in its mount, and observing the precession of the laser spot at some distance (30-40') from the source. Performing this evaluation yields a pointing accuracy for the HeNe of 160-180 micro-radians, which is acceptable as a standard for calibrating the system.

The far field portion of the calibration apparatus is illustrated in Figure 11, and consists of a plate on a movable stand that has two 0.06" diameter holes drilled in its face (these holes are too small to be visible in Figure 11). The separation distance

Figure 11. Alignment fixture constructed to ensure accurate calibration of the fast and slow scan mirror position. Assembly will be bolted to the cement floor for long term stability.

between these holes is the same as that between the HeNe and the scanner, when the scanner is "looking" directly forward and the beam propagation direction is horizontal. Using these fixtures, we can accurately position the beam scan mirrors (with the scan motors turned off) and then read the respective encoder values for each scan axis relative to the encoder index pulse. Assuming none of the optics move after this calibration is performance (we believe this will be a good assumption), this procedure will yield us a positional calibration of beam position to an accuracy of 200-300 micro-radians.

2.4.4. Heat Transfer

During measurement, the gasifier is under a slight vacuum, which results in an influx of ambient air through the measurement port of the gasifier. Thus, convective heat transfer will actually cool the instrument, and the primary mode of heat transfer will be via radiation from the hot gasifier wall.

Assuming the following:

Gasifier wall temperature:	1360 °K
Head surface area:	0.066 m^2
Head surface emissivity:	0.4
Unity view factor	

The total heat flux to the head will be approximately 77,500 W/m^2. This equates to a cooling requirement of 0.75 gal/min, allowing for a 30 °K difference between the inlet and outlet cooling water temperatures. Given the low flow rates, there is considerable margin of safety to account for increases in surface emissivity and or variation in gasifier wall temperature that cooling the unit should not pose a significant problem.

Heat transfer to internal components through the windows must also be minimized to prevent overheating and optical alignment drift caused by thermal expansion of the mounting structure. Our prior experience suggests that adequate thermal filtering cannot be accomplished using a single optic. To do so places an unacceptably high thermal load on the window, usually resulting in failure due to thermal stress. The problem is better solved by dividing the heat load between multiple pieces of glass, each tuned to reflect or absorb a portion of the thermal load. Thus, the "window" is actually a multi-element assembly consisting of:

1) A Schott glass window.
2) A hot mirror, which reflects all energy between 760-1500 nm
3) A standard BK7 glass window that absorbs long wavelength thermal radiation, as well as acts as a sealing surface.

2.4.5. External Mount

Gasifier measurements require a mounting extension to position the scanning head at the proper location inside the gasifier. This unit, shown in combination with the head in Figure 12, consists of a water-cooled annulus that at one end mounts to the scan head, and has appropriate fixturing attached to position the unit accurately relative to the gasifier's burner nozzle port. The fixturing is actually in two parts: a base plate is placed over the bolt pattern on the gasifier's

burner port, and a mating flange that is permanently attached to the external mount. This will allow rapid insertion and extraction of the device during measurement of the hot gasifier.

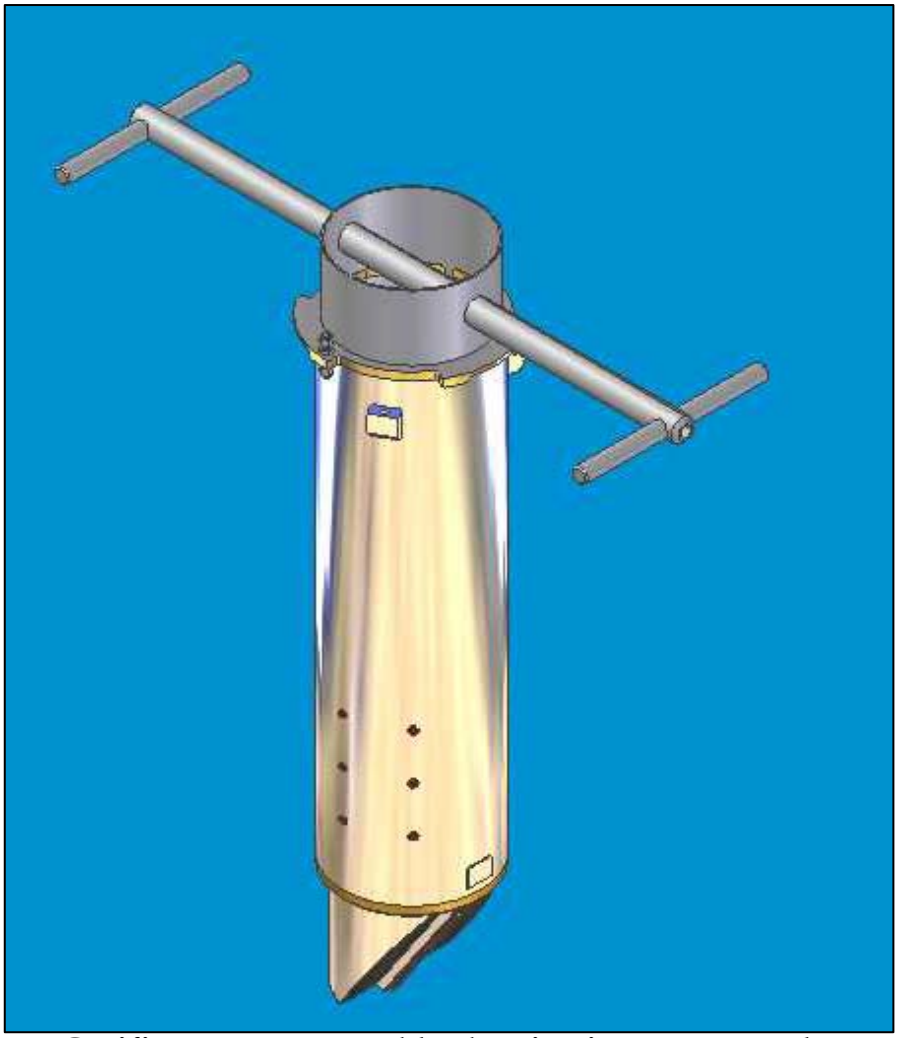

Figure 12. Gasifier scanner assembly showing instrument and external mount in the inverted position, ready for measurements in the gasifier. Handles at the top allow insertion and extraction.

2.5. Software

This section below describes the design and implementation of the Software that controls the PMC LCS laser scanning head. Development is done with Microsoft Visual C++ 6.0. The software was designed to run as a single console application on Windows XP professional.

2.5.1. Design

Method: Object Oriented and Top Down methods for software design were used throughout the design process. The major components of the LCS were identified (see table 1) and software classes that encapsulate/control each of these components were designed and implemented. The major components identified were: IO Card, Acuity Card, Slow Motor, Inclinometer, Communications (To LCS, other systems) and the Scanning Head itself (as single unit/component).

Table 1. Major LCS components and associated C++ class name.

Component	Class	Base Class
National instruments IO Card	NIPCI6221Controller	IOCardController
Acuity Card	AcuityCardController	
Faulhaber Brushless ServoMotor	FaulhaberController	SlowMotorController
VTI-Technologies Inclinometer	VTITechInclinometerController	InclinometerController
Communications (To LCS, other systems)	CommunicationsController	
LCS Head (Whole System)	PMCLCSHeadController	

Since some of the components might be changed or purchased from different vendors in the future base classes encapsulating the basic operation and functions of these components have been designed and implemented to make the software easier to maintain and enhance. Then specific classes for the particular component used in the system were derived from the base classes. For example, as indicated in Table 1 base classes were developed for IO cards , slow motors and inclinometers. The specific classes were derived from the respective base classes for the National Instruments IO card, Faulhaber ServoMotor and VTI-Technologies inclinometer.

Implementation:
Figure 13 shows the basic architecture of the laser scanning head.

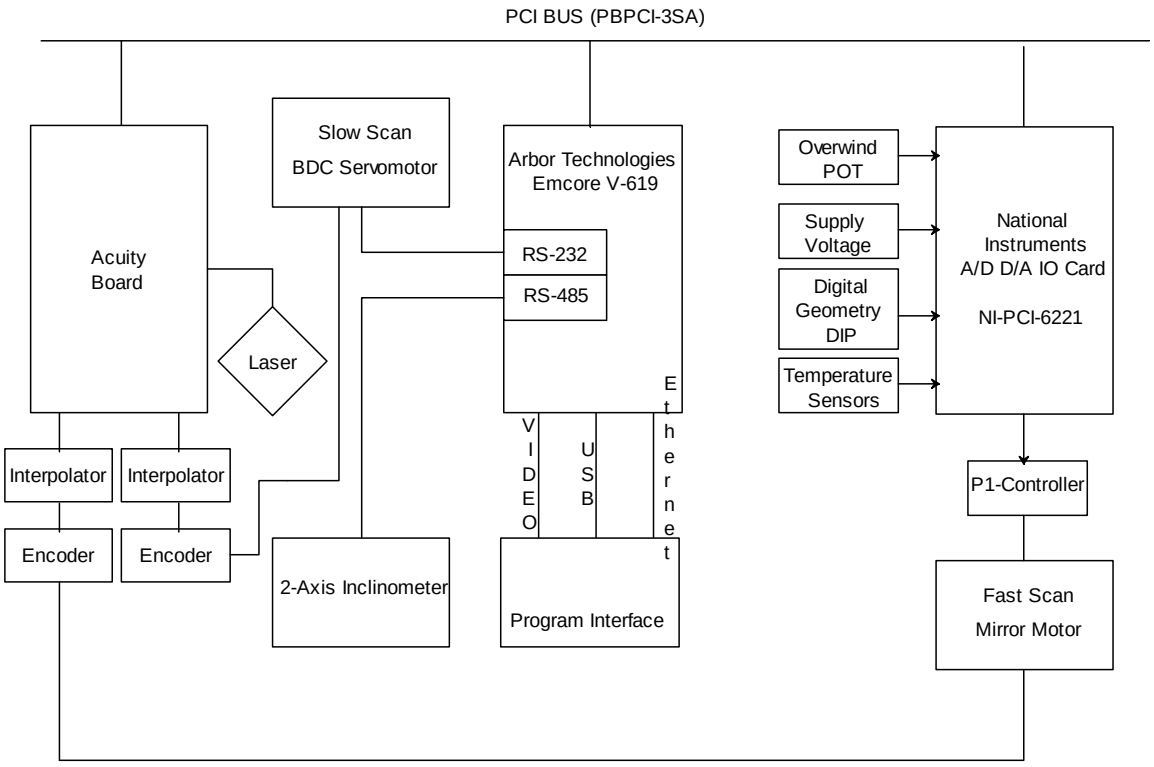

Figure 13. Architecture of the components that comprise the range finder.

Individual components are described as follows:

- The IO card controller is used to read (through the A/D input channels) the over-wind potentiometer, power supply, digital geometry DIP and temperature sensors. It is also used to control the fast scan motor by supplying (through the D/A channel) the control voltage to the P1 controller that controls the motor.

- The Acuity card controller controls the laser and feed the range data along with the encoder values for both the fast and slow scan motors to the head controller.

- The slow motor controller is used to control the speed and position of the slow motor through the RS-232 serial communications port.

- The inclinometer controller is used to read the inclination angles of the inclinometer.

- The communication controller is used to communicate with the outside word (in this case the LCS computer). It listens for requests to establish a communication link with the head, parses and validates incoming

requests and commands and sends back the scan data and /or status information to the outside world.

Each of these controllers uses multiple threads in order to achieve asynchronous communication between itself the hardware it controls and the main head controller.

The head controller contains one of each of the above controllers and uses them to control the operations and functioning of the scanning head. It first initializes itself and all the components (described above) it contains and then it waits for requests and commands coming in through the communications component. When the scan command comes in it performs the right pre-scanning computations, positions the head at the starting position and starts the scan. While scanning it collects the scanned data from the Acuity card, parses it, converts it to the right format and then sends the back to the outside world through the communications component.

2.6. Evaluation of PC-Board-Level Electronics from Acuity Technologies

After Process Metrix received the modified receiver and receiver power supply boards from Acuity Technologies, the boards were integrated with the transmitter/receiver and range measurements made with a test program to assess sensitivity to targets of various reflectivity and range accuracy. The following discusses the results of this analysis

2.6.1. Range accuracy

After aligning the detector with the receiver optics, data sets were collected to assess range accuracy. Figure 14 presents a series of 5000 range measurements made on a black felt target approximately 2.05 m from the transmitter receiver. After data collection, the data were sorted by range value and plotted as shown in Figure 14.

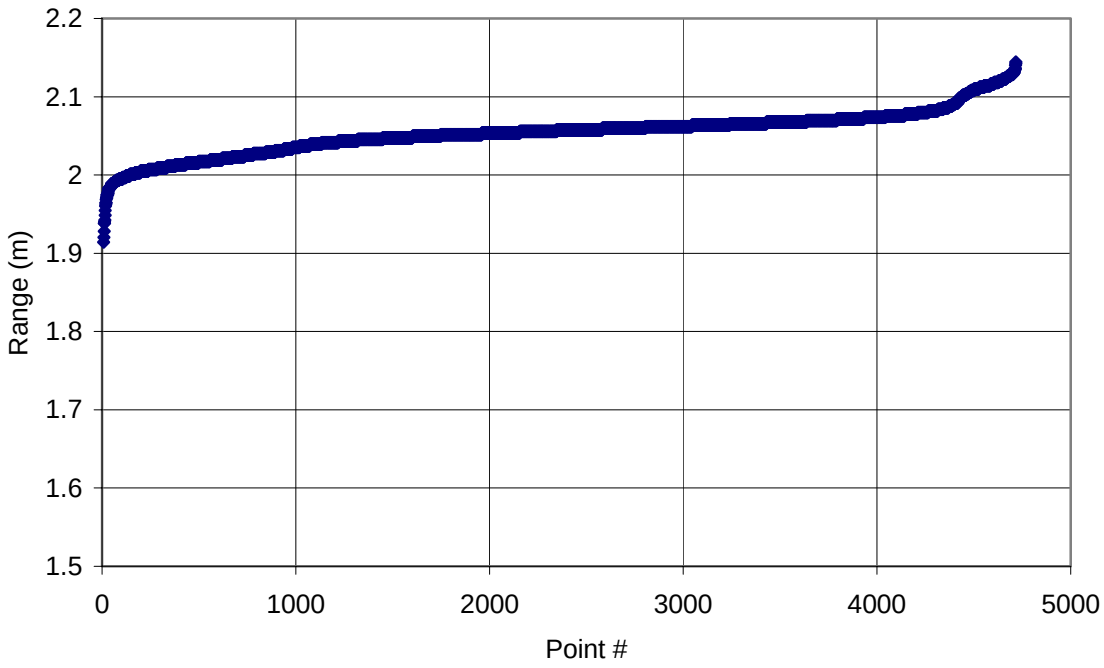

Figure 14. Ordered range values measured on a black felt target at a mean distance of 2.05m from the transmitter/receiver.

The data set has the following statistical characteristics:

Table 2. Statistical properties for data of Figure 14.

Parameter	All Data	Central 3000 Points
Std. Dev.	27.3	9.1
Mean	2,053.9	2,057.9
Mode	2,061.6	2,061.6
Median	2,057.6	2,057.6
Max	2,144.5	2,073.8
Min	1,914.1	2,037.4

Clearly, for the entire data set, the tails of the distribution shown in Figure 14 are problematic and weight the standard deviation and max/min of the data considerably. Eliminating the tails of the distribution and statistically considering only the central 3000 data points yields the data shown in the rightmost column of Table 1. For these data, the standard deviation as fallen to 9.1 mm, though the min/max is still larger than what we'd hope for in the final instrument.

What is causing the measurement noise? There are several possible sources of noise in the system. The first is APD noise, which is currently used to set the gain of the APD. All APD's exhibit gain functions that are highly sensitive to device temperature. In order to stabilize the gain, the system firmware monitors the noise data rate and adjusts the APD gain to keep the noise data rate at a constant value of approximately 24 kHz. While may seems excessive, since the laser timing window is small relative to the pulse period, the actual number of noise pulses detected during each range measurement is less than 0.2 Hz. Nevertheless, for a complete measurement consisting of 300000 data points, this translates to approximately 1200 erroneous range values – too many erroneous values for accurate measurement of lining thickness in the gasifier.

Other sources of noise include the detector itself, the gain electronics, and the timing circuit. Pending the outcome of our search for an alternate detector electronics package, we will begin evaluating the system for these alternate sources of noise in the next reporting period.

2.6.2. Detector Sensitivity

We also investigated sensitivity to various surface reflectivities at a range of 6.6 m (the largest range value we can easily configure in our current lab configuration). At this range, the system was able to measure returns from the following surfaces (in approximate order of decreasing reflectivity):

- Polished aluminum
- Bare aluminum
- Dull anodized aluminum (normal incidence)
- Used refractory brick sampled from a ladle used in the steel industry
- Steel slag (non-glassy)
- Black velvet
- Dull anodized aluminum (45° incidence).

We estimate that the dull, anodized aluminum at 45° incidence has a reflectivity of approximately 5% - 6%[1] and the black velvet approximately 8-9%[1]. The fact that we can easily range off of these surfaces suggests that we should be able to do the same in the gasifier. The only challenge may be on glassy slags. We hope to obtain a glassy slag sample from the steel industry and evaluate the range finders sensitivity to this surface at varying degrees of incidence as well.

The fact that we could range off of these surfaces with additional gain available raises the questions of whether or not an APD is necessary as a detector. If a high speed, silicon photo-diode could be substituted for the APD the noise issues

noted earlier could be solved without the more complicated implementation of a thermo-electric cooler.

2.7. Critical Electronics Evaluation and Decision for Re-Design

Through this point in the project, a functional optomechanical system had been developed that could be used to make range measurements absent the scanner element of the system. However, a principle hurdle has not been overcome; namely the reduction of range measurement uncertainty to ~8 mm, the milestone target stipulated in our original proposal. After extended discussions with Acuity Research, it was no longer clear that they would be able to produce an electronics package capable of meeting our requirements. The hurdles were too large, and Acuity's capabilities in the area of high speed electronics limited in scope and experience.

Process Metrix subsequently searched out other vendors that produce state-of-the-art detection electronics necessary to process accurate range measurements. The expertise embodied in this area goes well beyond simple pulse detection, but also includes: 1)pulse analysis to reduce range error (commonly known as range "walk"), 2) long term timing stability, 3) ongoing improvements in high speed time-to-digital converter technology, and 4) detector noise minimization through the combination of cooling and/or appropriate circuit design.

Throughout these discussions, Process Metrix repeatedly assessed whether or not we should take on our own development starting either from scratch or by using part of the electronics package supplied to us by Acuity Technologies. In each case, we arrive at the same conclusion: The investment required to reinvent the knowledge base that already exists would require a significant time and resource. Furthermore, we may find that our in-house product is still inferior to the state-of-the-art technology that is constantly being improved by the vendors that we have talked with whose primary commercial product is range finder technology.

Unfortunately, reliance on external sources for a key element of the range finder design also leaves the project susceptible to time delays that are outside our control. The technology required to achieve or exceed the measurement uncertainty milestone will require state-of-the-art electronics that are not an off-the-shelf item and, will require a significant investment of resource by Process Metrix. While this investment would not be born by project funds, we recognized that this core element must be within PMC's control, and we undertook the development internally.

2.8. Re-Design, Test and Evaluation of Range Finder Electronics

2.8.1. Time-to-Amplitude Converter (TAC)

Overview

A consultant with 30 years experience in the nuclear physics industry was retained to assist with the development of an overall system architecture and appropriate circuit design. Through the first three quarters of 2007, circuit designs were developed and modeled using our Altium design tool until the timing circuit demonstrated acceptable performance in the modeled environment. This design was subsequently developed into a working prototype, and evaluated late in the third quarter of 2007. Testing confirmed performance as predicted by the model, and we now have a Time-to-Amplitude converter (TAC) capable of 3 picosecond timing accuracy.

The Time to Amplitude Converter (TAC) is a subsystem that converts two discrete electrical events in time to a high precision proportional voltage that is input to an analog-to-digital converter (ADC). The output of the ADC is passed to a computer for processing. For this application, the time events are generated by a pulsed laser. A packet (~2-5 nanoseconds) of pulsed laser light is fired at a target up to 50 meters away. The time required for the light to travel from the emitter and back to the receiver is precisely represented by a corresponding voltage in the TAC.

Note: *Range* is defined by total round trip light time-of-flight divided by two e.g. 50 meters target range requires the light to travel 100 meters total.

TAC Function

The TAC is driven by a start /stop pulse consisting of a complementary rising (start) and a falling (stop) voltage waveform generated by a constant fraction discriminator. The difference in time (Δt) between the start and stop pulse is determined by the time taken by the photons in the laser pulse to exit from and return to the optical system. The simplified schematic and timing diagrams for the TAC are illustrated in Figure 15.

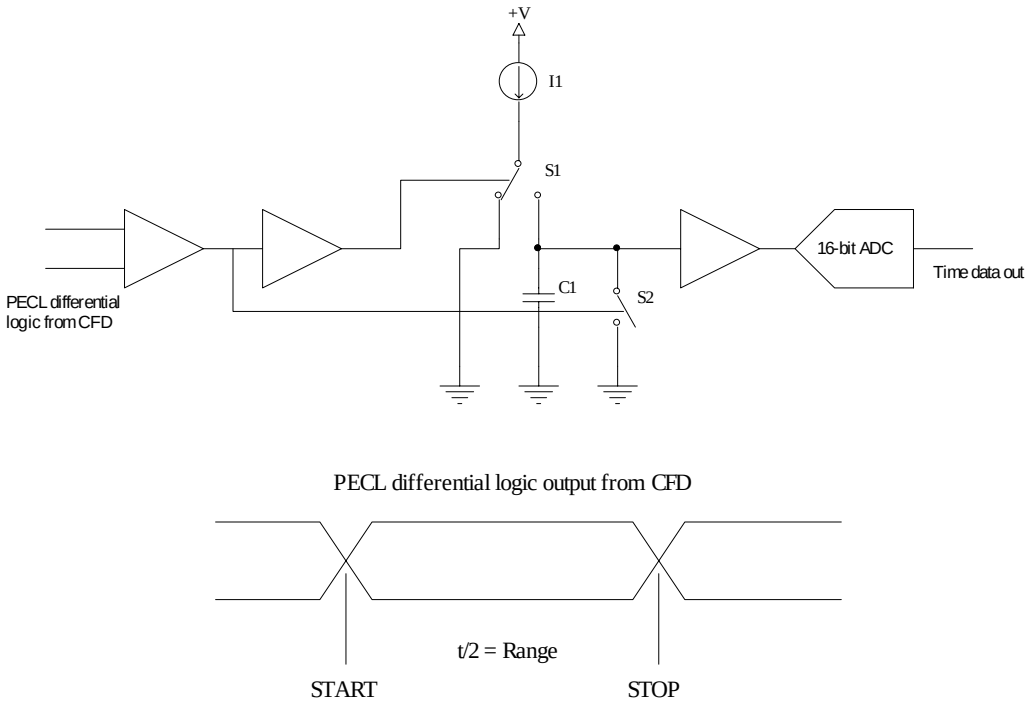

Figure 15. TAC concept

While waiting for the start pulse the TAC remains ready and reset (condition (a) in Figure 16 below). Upon the start event, current from a constant source is switched into a capacitor which charges linearly (condition b). When the stop pulse arrives, the current source is switched away from the capacitor and it stops charging (condition c). The voltage charge on the capacitor holds and proportionally represents Δt. The voltage across the capacitor is sampled and digitized by a 16-bit analog-to-digital converter. After ADC sampling, the capacitor is reset by shorting it to ground and is ready for the next cycle (condition a). A complete TAC charge/reset cycle is illustrated in Figure 17.

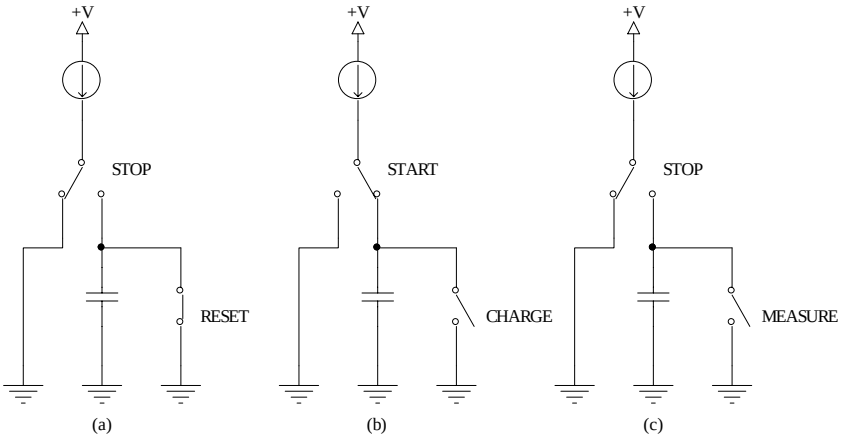

Figure 16. Operational cycle of the TAC.

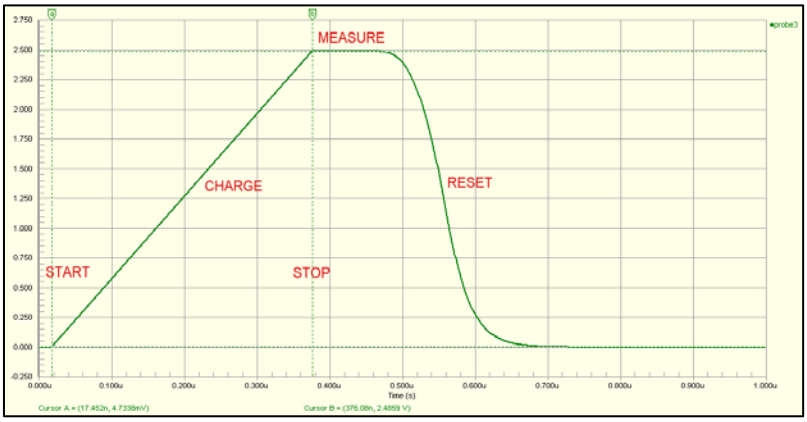

Figure 17. TAC Cycle.

Figure 18 illustrates ADC output as a function of capacitor charge time. High linearity of the output is essential for accurate operation of the TAC.

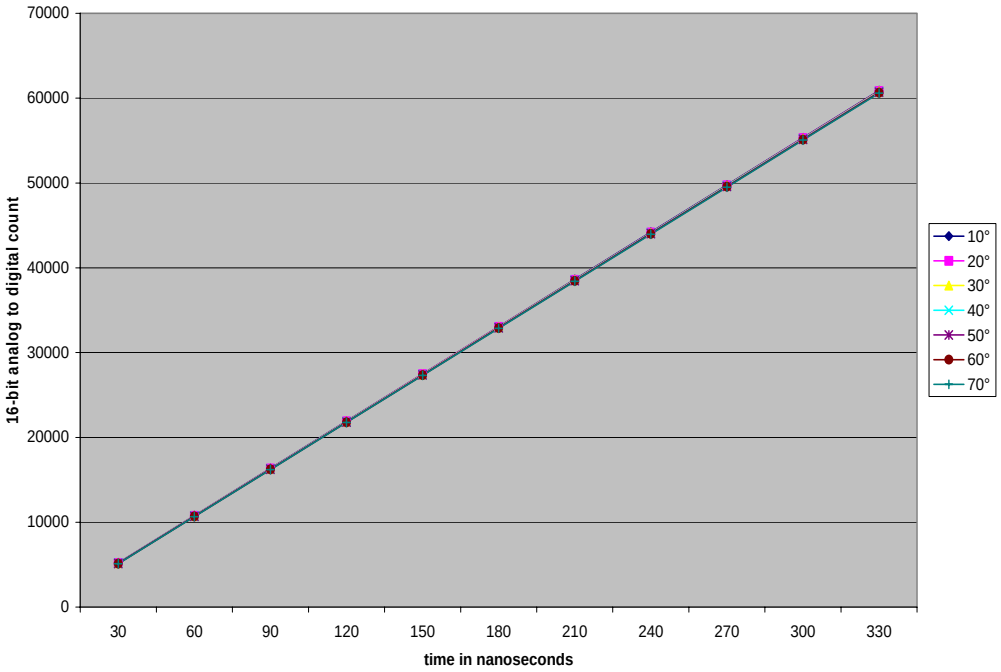

Figure 18. Raw ADC counts versus time.

The capacitor charge function is given as follows:

$$V = C * Q$$

where: **V** volts
C capacitance in farads
Q charge in coulombs (ampere seconds)

The TAC can operate up to 200kHz and is only limited by laser pulse repetition rate and downstream processing electronics. The expected operational range of the TAC is from 1.5 to 50 meters. Other applications

may require more or less range and/or resolution; minor modification to the capacitor / current source make this a straightforward adaptation.

The minimum measurable distance is dictated by the pulse receiving circuitry. More specifically, by the time needed to reset the detection electronics after receiving the start pulse. We estimate that 12-16 ns will be required for re-set, which implies a minimum standoff distance of 6-8 feet. While this is acceptable for most surfaces in the gasifier, there may be limitations making measurements in the dome smaller units. In this case, fiber-coupling the return signal could be implemented to artificially introduce the required time delay between the start and stop pulses, thereby reduced the minimum standoff distance to practically zero.

Additionally, the TAC contains a time reference circuit which is used to internally generate precise start/stop pulses. From an external controller command, precise pulses of 30, 60, 90, 120, 150, 180, 210, 240, 270, 300, 330, 360 nanoseconds can be produced. The time base crystal is a precise, temperature stable oscillator.

Hardware

The TAC board and TAC testing board are illustrated in the figures below:

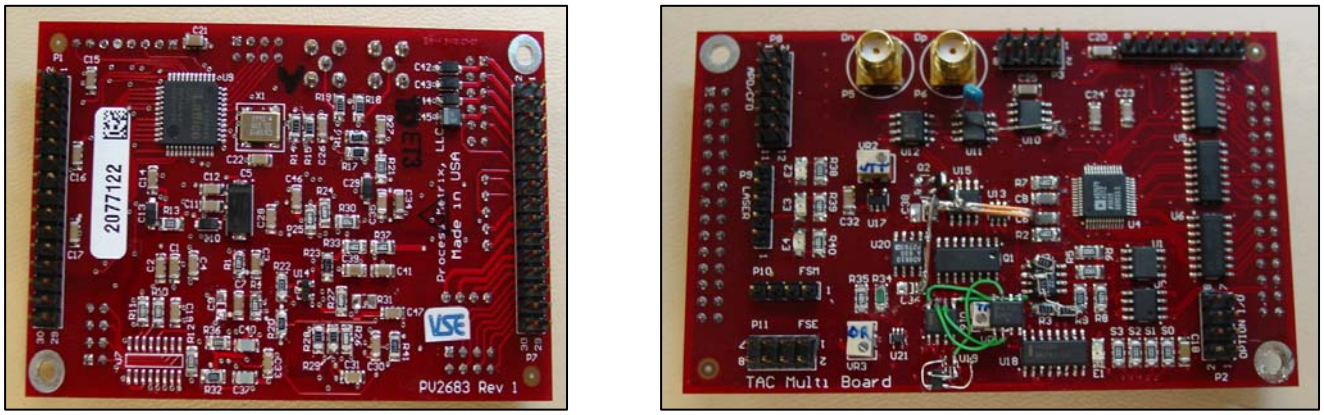

Figure 19 (a, left) TAC board – top and (b, right) TAC board – bottom.

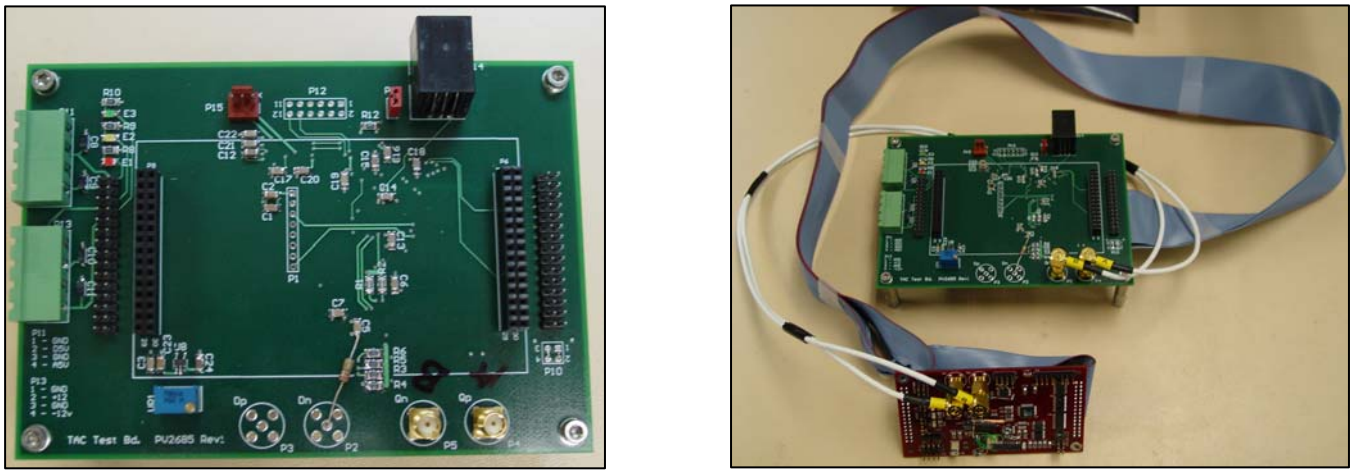

Figure 20 (a, left) TAC test board and (b, right) TAC board and TAC test board connected.

TAC Testing

In order to drive and test the TAC system a TAC test board was constructed. The TAC test board consists of a microcontroller, a time reference circuit, drive circuits, and an RS-232 interface for PC computer control and monitoring.

The microcontroller is programmed to receive configuration commands from the PC and drive the TAC board with a series of time reference pulses from both the TAC test board and the TAC board itself. A separate time reference was incorporated into the TAC test board so the performance of the time reference circuit on the TAC board could be evaluated under various temperature

conditions. This measurement could subsequently be compared to the temperature-stable output of TAC test board. Using two identical time references, the stability of the system and ability to compensate for any changes over temperature can be characterized.

The TAC test board and TAC board were exercised through a series of time measurements using the on-board time reference circuits under a temperature sweep from 10° to 70° C. The TAC board and TAC test board each contain a digital thermometer IC so temperature data could easily be collected from each circuit. The systems were wired together with ribbon cable and high frequency coax to allow independent temperature testing.

Figure 21 illustrates temperature sweep of the TAC board while the TAC test board temperature remained nominally constant. The system was programmed to take 10 samples at each time reference setting (30 to 330nS) and again at each

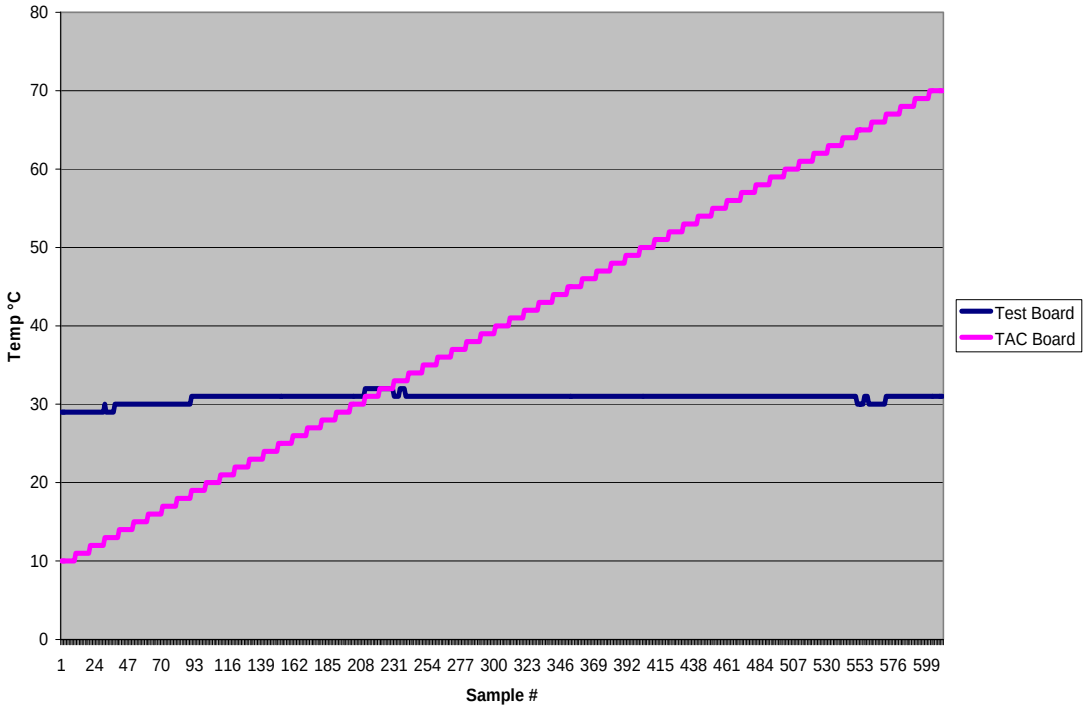

Figure 21. Temperature sweep of TAC board.

temperature level between 10° to 70°. These samples were averaged and are plotted in Figure 22.

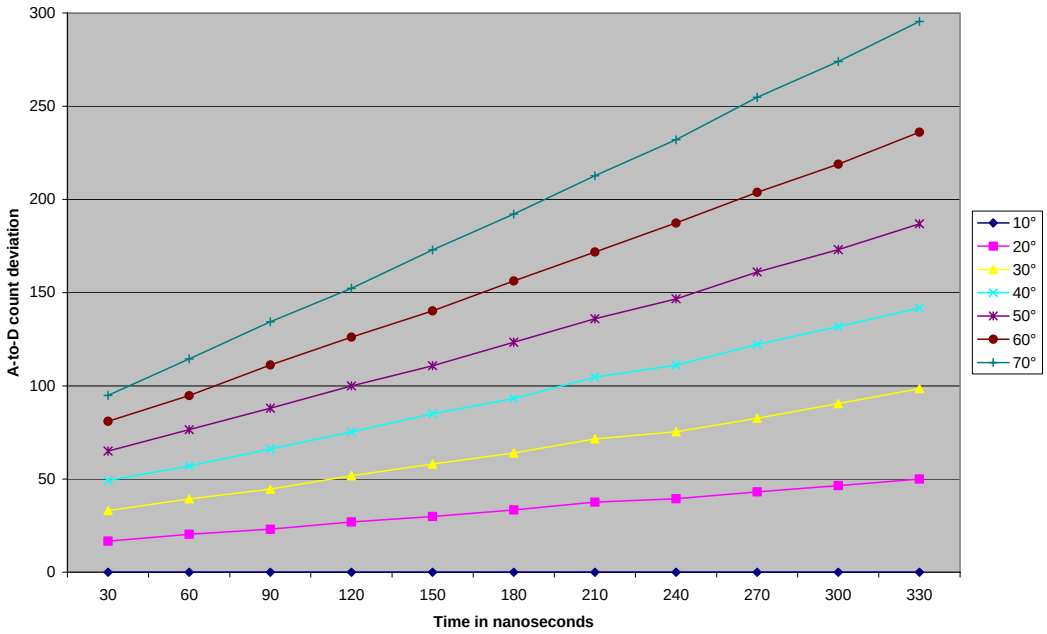

Figure 22. Relative difference in counts over temperature

relative ADC counts. Figure 22 demonstrates the thermal susceptibility of the deviations in the constant current source. Other factors over time could include aging of the TAC charge capacitor. This is the specific reason for the time reference circuit; on board calibration minimizes the need for strict stability requirements.

The time reference is built around a highly precise and thermally stable oscillator. It has a rating of ±25ppm over a -20 to 70 °C range. This translates to a maximum frequency deviation of 1/(33.333MHz - ±833.325Hz) - 30nS ≈ ±1ps. The specification also calls out a nominal period jitter spec of 3ps. The range uncertainty approximates to (±1ps + 3ps) * 0.3mm / 2 ≈ ±1.2mm.

Calibration

Using two-point calibration equations the ADC counts can be resolved in time (and range).

y = mx + c	calibration equation
m = (y2 – y1) / (x2 – x1)	slope
c = (y1 * x2 – y2 * x1) / (x2 – x1)	offset

where **m** = slope
c = offset
y = known values in time
x = unknown measurement (ADC count)

Range Measurement

Once the ADC counts are resolved in time, range measurement can be evaluated. For this exercise range is given by:

$$\mathbf{O = t * 300mm / 2}$$

where **O** = Range
t = calculated round-trip time

Relative range values for each time reference point were plotted through the temperature span, and are shown in Figure 23.

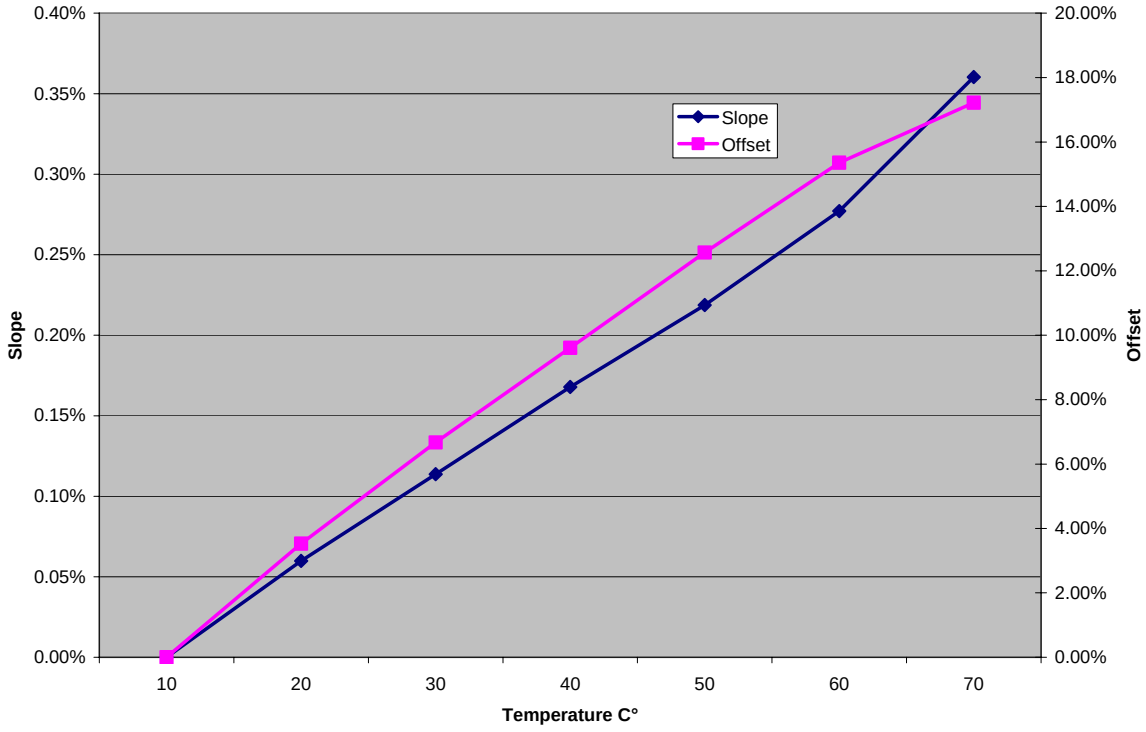

Figure 23. Relative difference in range over temperature calibration applied for each temperature.

Calibration slope and offset must change over temperature. Figure 24 illustrates the difference in compensation.

Non-Linearity

The non-linearity of the system in Figure 24 has been shown in Spice circuit modeling to be an artifact of inadequate base drive of the current steering TAC transistors. A new circuit has been devised and tested in Spice that will improve on these results and perform better over temperature. With this circuit however, some improvement in linearity over a limited measurement range can be made by simply changing the calibration points.

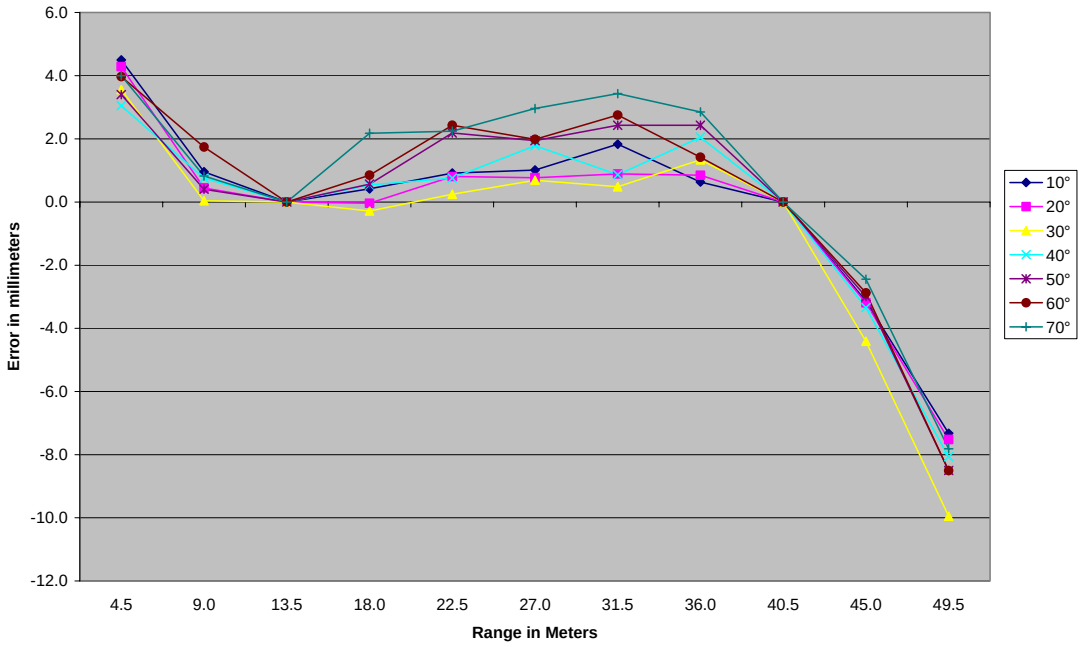

Figure 24. Calibration constants over temperature

Conclusion

The TAC system demonstrated good linearity over temperature and improvement in measurement quality is achievable. While slope and offset drift is large it can be measured with use of integrated reference time base and corrected. The reference time base is not affected by temperature change and is a good basis for an on-board calibration subsystem. The achievement of this level of performance represents a crucial milestone in this project; without this capability the project could not continue. Perhaps more importantly, the TAC's performance follows the predictions of the model. This gives us confidence we can continue to predict circuit performance with reasonably surety.

2.9. New System Architecture

In parallel with the circuit design, we've also completely redesigned the system architecture. The core element is the laser; subsequent to our earlier calculations we've now concluded that operating in the visible wavelength range could leave us susceptible to particle scattering. Since we don't yet have the ability to detect more than one return signal per laser pulse (we're working on this problem as well), a return from a particle cloud effectively nullifies that range value for that laser pulse.

In the last 18 months there have been significant advances in passively Q-switched laser technology, and there are now a number of vendors that offer lasers with 100 kHz repetition rates at higher than 1 kW (peak) output power. We've modified the design of the transmitter to incorporate a laser from Germany that can operate at 100 kHz. This 8x speed improvement will shorten the measurement time and reduce the incident heat load on the device during data collection when the gasifier is near operating temperature.

Increasing the laser repetition rate also requires faster mirror rotation rates and data acquisition. Fortunately, the mirror motors we originally selected can achieve the higher speed requirements, though the data processing must be completely re-worked to operate at higher throughput. In the latter case we are switching from the on-board computer configuration proposed initially to digital signal processing (DSP) and have retained a separate consultant to source the hardware and write the firmware necessary to acquire the data. We will incorporate the Rabbit microprocessor (this device is well know to us that we use it in several different product lines) for Command and Control and to transfer the data from the DSP to a standard PC (laptop) for data reduction and file storage.

3. SUMMARY

Process Metrix began this project with the intent of modifying an existing ranging system and combining the same with a specially designed optical scanner to yield three dimensional range images that could be used to determine the refractory lining thickness in a gasifier. The goal was to make these measurements during short outages while the gasifier was at or near operating temperature.

Our initial estimates of the photon counts needed for the modulation-based range finder were optimistic, and we were forced to undertake a redesign of the range finder portion of the project. This ultimately created significant and unanticipated time delays that were exacerbated when Acuity Technologies, the subcontractor responsible for delivering the redesigned range finder, failed to deliver electrical components capable of meeting the specific range error requirements needed for accurate lining thickness measurement. An extensive search for an alternate, off-the-shelf solution was unsuccessful, and Process Metrix was forced to undertake the electronics development internally without project funds.

The positive outcome of this effort is a documented set of range finder electronics that have exceptional accuracy, simplicity, temperature stability and detection limit; in sum a package perfectly suited to the measurement requirements and

within our control. It is unfortunate yet understandable, given the time delays involved in reaching this milestone, that the Department of Energy decided not to continue the project to completion. The integration of this electronics set into the optomechanical hardware also developed within the scope of the project remains as follow-on project that Process Metrix will finish within the calendar year 2008.

Testing in the gasifier is, at this point, not certain pending the award of additional funding needed for field trials. Eastman, our industrial partner in this project, remains interested in evaluating a finished system, and working together we will attempt to secure funding from alternate sources that have been referenced by our contract monitor. It remains our hope and goal to follow this project through to completion, thereby achieving the objectives outlined at the start of our effort.

4. APPENDIX

4.1. Component and vendor information

The manufacturer of the PC104 computer board and the backplane is a company called Arbor Technology and it is located in Taiwan.
http://www.arbor.com.tw

The board is the Emcore-V619:
http://www.arbor.com.tw/half-size/emcore-v619.htm

PCI Backplane:
http://www.arbor.com.tw/peripherals/pbpci-3sa.htm

The PC104 SBC board is actually bought from Global American Inc; Product Number 3301121:
http://www.globalamericaninc.com/new_spec/spec2.php?id=396

The PCI bus (3 slots) is also from Global American Inc; Product Number 1107645:
http://www.globalamericaninc.com/backplanes/pci_bp.php

The National Instruments card is the PCI6221:
http://sine.ni.com/nips/cds/view/p/lang/en/nid/14132

The Acuity card is a custom made card made from Acuity Techologies:
http://www.acuitytx.com/
http://www.acuitytx.com

The Slow Motor and Controller are bought from Faulhaber (US distributor MicroMo Electronics):
http://www.micromo.com/

Motor: 3564 K 024 B K 1155:
http://www.micromo.com/library/docs/products/eBLM3564.pdf

Controller: MCBL2805:
http://www.micromo.com/library/docs/products/eMCBL2805.pdf

The Inclinometer is from VTITech:http://www.vti.fi/en/index.html
Product is SCA125T:
http://www.vti.fi/productsen/productsen_2_1_4_1.html

4.2. List of files developed/integrated in project:

1) Header files

AcuityCardController.h
CommunicationsController.h
DriverInterface.h
FaulhaberController.h
GSSI.h
GSSIDef.h
hw_sup.h
InclinometerController.h
InstrumentServer.h
InstrumentSocket.h
IOCardController.h
MathUtil.h
NIDAQmx.h
NIPCI6221Controller.h
PMCLCSHead.h
PMCLCSHeadConstants.h
PMCLCSHeadController.h
PMCLCSHeadMacros.h
PMCLCSHeadStructures.h
PMCLCSHeadUtil.h
pstdll.h
range.h
Resource.h
SerialCommControl.h
SerialCommController.h
SlowMotorController.h
StdAfx.h
sys_funcs.h
VTITechInclinometerController.h

2) C++ files

AcuityCardController.cpp
CommunicationsController.cpp
FaulhaberController.cpp
InclinometerController.cpp
InstrumentServer.cpp
InstrumentSocket.cpp
IOCardController.cpp
MathUtil.cpp
NIPCI6221Controller.cpp

PMCLCSHead.cpp
PMCLCSHeadController.cpp
PMCLCSHeadUtil.cpp
pstdll.cpp
range.cpp
SerialCommControl.cpp
SerialCommController.cpp
SlowMotorController.cpp
StdAfx.cpp
sys_funcs.cpp
VTITechInclinometerController.cpp